

ORIGINAL RESEARCH ARTICLE

# Gut Microbiota–Derived Trimethylamine N-Oxide Contributes to Abdominal Aortic Aneurysm Through Inflammatory and Apoptotic Mechanisms

Tyler W. Benson, PhD<sup>\*</sup>; Kelsey A. Conrad, PhD<sup>\*</sup>; Xinmin S. Li<sup>1</sup>, PhD; Zeneng Wang<sup>1</sup>, PhD; Robert N. Helsley<sup>1</sup>, PhD; Rebecca C. Schugar, PhD; Taylor M. Coughlin<sup>1</sup>, BS; Caris Wadding-Lee<sup>1</sup>, BS; Salma Fleifel<sup>1</sup>, BS; Hannah M. Russell, PhD; Timothy Stone<sup>1</sup>, PhD; Michael Brooks, BS; Jennifer A. Buffa, MS; Kevin Mani, MD, PhD; Martin Björck<sup>1</sup>, MD, PhD; Anders Wanhainen, MD, PhD; Naseer Sangwan, PhD; Sudha Biddinger, MD; Rohan Bhandari<sup>1</sup>, MD; Akiirayi Ademoya, BS; Crystal Pascual, BS; W.H. Wilson Tang<sup>1</sup>, MD; Michael Tranter<sup>1</sup>, PhD; Scott J. Cameron<sup>1</sup>, MD, PhD; J. Mark Brown, PhD; Stanley L. Hazen<sup>1</sup>, MD, PhD; A. Phillip Owens<sup>1</sup> III, PhD

**BACKGROUND:** Large-scale human and mechanistic mouse studies indicate a strong relationship between the microbiome-dependent metabolite trimethylamine N-oxide (TMAO) and several cardiometabolic diseases. This study aims to investigate the role of TMAO in the pathogenesis of abdominal aortic aneurysm (AAA) and target its parent microbes as a potential pharmacological intervention.

**METHODS:** TMAO and choline metabolites were examined in plasma samples, with associated clinical data, from 2 independent patient cohorts (N=2129 total). Mice were fed a high-choline diet and underwent 2 murine AAA models, angiotensin II infusion in low-density lipoprotein receptor–deficient (*Ldlr*<sup>−/−</sup>) mice or topical porcine pancreatic elastase in C57BL/6J mice. Gut microbial production of TMAO was inhibited through broad-spectrum antibiotics, targeted inhibition of the gut microbial choline TMA lyase (CutC/D) with fluoromethylcholine, or the use of mice genetically deficient in flavin monooxygenase 3 (*Fmo3*<sup>−/−</sup>). Finally, RNA sequencing of in vitro human vascular smooth muscle cells and in vivo mouse aortas was used to investigate how TMAO affects AAA.

**RESULTS:** Elevated TMAO was associated with increased AAA incidence and growth in both patient cohorts studied. Dietary choline supplementation augmented plasma TMAO and aortic diameter in both mouse models of AAA, which was suppressed with poorly absorbed oral broad-spectrum antibiotics. Treatment with fluoromethylcholine ablated TMAO production, attenuated choline-augmented aneurysm initiation, and halted progression of an established aneurysm model. In addition, *Fmo3*<sup>−/−</sup> mice had reduced plasma TMAO and aortic diameters and were protected from AAA rupture compared with wild-type mice. RNA sequencing and functional analyses revealed choline supplementation in mice or TMAO treatment of human vascular smooth muscle cells–augmented gene pathways associated with the endoplasmic reticulum stress response, specifically the endoplasmic reticulum stress kinase PERK.

**CONCLUSIONS:** These results define a role for gut microbiota–generated TMAO in AAA formation through upregulation of endoplasmic reticulum stress–related pathways in the aortic wall. In addition, inhibition of microbiome-derived TMAO may serve as a novel therapeutic approach for AAA treatment where none currently exist.

**Key Words:** aortic aneurysm, abdominal ■ endoplasmic reticulum stress ■ gastrointestinal microbiome ■ PERK kinase ■ trimethylamine

**A** bdominal aortic aneurysms (AAAs) are focal dilations of the abdominal aorta, often occurring in the segment of the aorta below the kidneys, and are clinically defined as an infrarenal aortic diameter of ≥3.0 cm.<sup>1</sup> AAAs affect 5% to 10% of men and 1% of women >65 years of age, and are now the 13th leading

Correspondence to: A. Phillip Owens III, PhD, University of Cincinnati, 231 Albert Sabin Way, ML: 0542, Cincinnati, OH 45267-0542. Email [phillip.owens@uc.edu](mailto:phillip.owens@uc.edu)

<sup>\*</sup>T.W. Benson and K.A. Conrad contributed equally.

Supplemental Material is available at <https://www.ahajournals.org/doi/suppl/10.1161/CIRCULATIONAHA.122.060573>.

For Sources of Funding and Disclosures, see page 1094.

© 2023 American Heart Association, Inc.

Circulation is available at [www.ahajournals.org/journal/circ](http://www.ahajournals.org/journal/circ)

## Clinical Perspective

### What Is New?

- Here, we demonstrate that disruption of the meta-organismal production of trimethylamine N-oxide (TMAO) by targeting either the gut microbiome or the liver enzyme flavin monooxygenase 3 of the host organism decreases circulating TMAO and protects mice from abdominal aortic aneurysm development in 2 independent mouse models.
- TMAO, not trimethylamine, drives abdominal aortic aneurysm pathogenesis, as demonstrated by flavin monooxygenase 3 knockout mice, which are protected from abdominal aortic aneurysm and have significantly increased trimethylamine but inhibited TMAO production.
- TMAO augments the unfolded protein response evident by increased expression of PERK, ATF5, and CHOP while also increasing caspase 3 activation and apoptosis in vascular smooth muscle cells.

### What Are the Clinical Implications?

- Our work introduces the gut microbiome and associated metabolites as novel mediators of abdominal aortic aneurysm.
- TMAO and associated analytes may serve as predictive biomarkers for both the incidence and growth rate of abdominal aortic aneurysms.
- Intervention with targeted nonlethal inhibitors of the gut microbiome provides us with new options for pharmacological treatment of aortic aneurysm.

cause of death in the United States (estimated at 15 000 deaths annually).<sup>2,3</sup> Likely prompted by a diverse array of initial injuries, the progression of AAAs is characterized by increases in inflammatory mediators, reactive oxygen species, matrix metalloproteinase activity, and vascular smooth muscle cell (VSMC) apoptosis, leading to progressive dilation and weakening of the aortic wall. Left untreated, progressive AAA dilatation often results in fatal rupture.<sup>4,5</sup> Currently, the only treatment option for patients with AAA is surgical intervention, pursued only when the risk of aneurysm rupture outweighs the risk of surgery.<sup>3</sup> Although many drugs have been investigated as potential therapeutics, none have consistently shown to attenuate AAA progression or rupture in humans.<sup>6–9</sup>

Until recently, dietary constituents were assumed to be absorbed in our intestine and metabolized by our resident human cells. In fact, the gut microbiome, a community of trillions of commensal organisms acting collectively as a metabolically active endocrine-like organ, is now known to contribute to host physiology through the digestion of macronutrients, vitamin synthesis, and generation of biologically active metabolites.<sup>10</sup> It is important to note that although the majority of the microbiome functions to propagate homeostasis, recent studies have dem-

## Nonstandard Abbreviations and Acronyms

<b>AAA</b>	abdominal aortic aneurysm
<b>ABX</b>	antibiotics
<b>AngII</b>	angiotensin II
<b>CHOP</b>	C/EBP homologous protein
<b>ER</b>	endoplasmic reticulum
<b>FMO3</b>	flavin monooxygenase 3
<b>GADD34</b>	growth arrest and DNA damage-inducible protein
<b>HAVSMC</b>	human aortic vascular smooth muscle cell
<b>OR</b>	odds ratio
<b>PERK</b>	protein kinase R-like endoplasmic reticulum kinase
<b>TMAO</b>	trimethylamine N-oxide
<b>UPR</b>	unfolded protein response
<b>VSMC</b>	vascular smooth muscle cell

onstrated that specific microbiota-derived metabolites can contribute to several cardiometabolic diseases.<sup>10,11</sup> Specifically, the microbiota-derived metabolite trimethylamine N-oxide (TMAO) has repeatedly been associated with and mechanistically linked to multiple cardiovascular diseases such as atherosclerosis and concomitant myocardial infarction, stroke, and heart failure.<sup>12–14</sup> TMAO has also been linked to metabolic diseases such as insulin resistance and type II diabetes, chronic kidney disease, obesity, and alcohol-associated hepatitis liver injury in both human and animal studies. Although the mechanisms of TMAO-induced increases in these disease states are still being investigated, this meta-organismal metabolite is known to induce reactive oxygen species, cytokine production, and profibrotic/inflammatory signaling pathways, in conjunction with the activation of platelets, endothelial cells, and VSMCs.<sup>12,13,15–21</sup> Despite extensive investigation of the gut microbiota (specifically, TMAO) in cardiometabolic diseases, a role for the TMAO meta-organismal pathway in AAA is vastly understudied.

Results from several recent publications suggest possible links of the gut microbiome to aneurysmal disease. For instance, TMAO levels predict long-term adverse event risk and mortality in patients with peripheral artery disease.<sup>22</sup> In addition, TMAO was associated with acute aortic dissection in a recent small case-control study using metabolomics to compare patients with acute aortic dissection with healthy control subjects.<sup>23</sup> Moreover, the gut microbiome facilitates angiotensin II (AngII)-induced vascular reactive oxygen species and hypertension.<sup>24,25</sup> The overall renin-angiotensin system, which is intimately linked to aneurysm disease pathology, has also emerged as a potential mediator of several microbiota-related effects through the local gastrointestinal renin-angiotensin system.<sup>26</sup> Thus, a recent study found that the

gut microbiome is markedly different when analyzed in mice with AAA versus controls.<sup>27</sup> To further examine the link between the gut microbiome and AAA, we demonstrate that plasma TMAO concentrations correlate with risk for AAA in 2 independent human cohorts, increased plasma TMAO exacerbates AAA formation in multiple murine models of AAA, and TMAO-driven AAA is likely mediated by enhanced activation of endoplasmic reticulum (ER) stress-related signaling.

## METHODS

Additional (full) detailed methods are presented in the [Supplemental Material](#). All raw data and analytical methods are available from the corresponding author on appropriate request.

### Mouse Study Approvals

All studies were performed under protocol 15-01-29-01 and continued with protocol 20-11-05-02 with approval and in accordance within the guidelines of the University of Cincinnati Institutional Animal Care and Use Program.

### Human Study Approvals

This study complies with the Declaration of Helsinki. All European research was approved by the research ethics review board of the Uppsala/Örebro region (authorization/protocol Dnr 2007/052). All North American research was approved by the Cleveland Clinic institutional review board (protocol 15834-2015). All participants (European and North American) gave written informed consent before their participation and sample collection. All patients and control subjects were of similar ethnic origin (European and White) and socioeconomic backgrounds.

### Statistical Analyses

All statistical analyses were performed with SigmaPlot version 14.5 (SPSS, Chicago, IL) or RStudio-R version 4.1.2 (2021-11-01; R Foundation for Statistical Computing, Vienna, Austria). Values of  $P < 0.05$  were considered statistically significant. Data are represented as mean  $\pm$  SEM. Data normality was assessed with a Shapiro-Wilk test. Two-group comparisons were performed with the Student  $t$  test (parametric) or Mann-Whitney rank-sum test (nonparametric). Multiple groups were compared with a 1-way ANOVA with Holm-Sidak post hoc analysis or, when normality could not be assumed, a Kruskal-Wallis test with a Dunn post hoc analysis using Bonferroni multiple-testing correction. To compare multiple groups with 2 independent variables, a 2-way ANOVA with Holm-Sidak post hoc analysis was used. Two-sided  $t$  tests were used to determine the significance of regression coefficients. Multiple Fisher exact tests were performed to compare each group pairwise for categorical values such as aneurysm incidence. When  $\geq 3$  independent treatments were present, aortic diameter data were fit to a linear regression model, with each individual treatment handled as a binary indicator to assess the overall effect of each applied treatment. To compare survival estimates, a log-rank test was performed with multiple comparisons by a post hoc Holm-Sidak test. The Wilcoxon rank-sum test or Welch

2-sample  $t$  test for continuous variables and  $\chi^2$  test or Fisher exact test for categorical variables were used to examine the difference between the groups. The Dunn test was used for pairwise multiple comparisons of the ranked data, and the Jonckheere-Terpstra test was used to test independent samples against ordered alternatives. Odds ratio (OR) for binary AAA and corresponding 95% CIs were calculated with both univariable (unadjusted) and multivariable (adjusted) logistic regression models. The logistic regression model was adjusted for traditional cardiac risk factors.

## RESULTS

### Elevated Plasma TMAO Is Associated With Increased AAA in Both the European and US Cohorts

We examined the clinical significance of TMAO levels with AAA risk in 2 independent AAA case-control cohorts of stable subjects undergoing cardiovascular evaluations. The European ( $n=352$ ; Uppsala, Sweden) and US ( $n=1777$ ; Cleveland, OH) cohorts who were collectively examined comprised a total of 2129 participants; the baseline clinical characteristics of each cohort are summarized in Tables 1 and 2. Participants who had AAA at enrollment in either the European cohort (learning cohort) or the US cohort (validation cohort) were older, had a greater prevalence of hypertension, used statins more frequently, and were more likely to be active smokers. In each cohort, we observed a significant association between higher TMAO concentrations and larger infrarenal abdominal aortic diameters (Kruskal-Wallis and Jonckheere-Terpstra test for increasing trend;  $P < 0.001$  each). Furthermore, plasma concentrations of TMAO were significantly elevated in participants with AAA (defined as a baseline aortic diameter  $\geq 3.0$  cm) versus control subjects (diameter  $< 3.0$  cm) in each cohort ( $P < 0.001$ ; Figure 1A and 1B). Compared with participants in the lowest quartile of TMAO levels, subjects in the highest quartile demonstrated a significantly increased odds for AAA in both the European cohort (quartile 4 versus 1: OR, 22.5 [95% CI, 10.6–51.3];  $P < 0.001$ ) and the US cohort (quartile 4 versus 1: OR, 2.1 [95% CI, 1.4–3.4];  $P < 0.01$ ). After multivariable logistic regression modeling to adjust for cardiovascular risk factors, including age, sex, smoking, hypertension, prevalent cardiovascular disease or coronary artery disease, medications, and indices of renal function, elevated TMAO levels remained independently associated with risk for AAA in both the European cohort (OR, 25.1 [95% CI, 10.7–63.4];  $P < 0.001$ ) and the US cohort (OR, 2.4 [95% CI, 1.1–5.1];  $P < 0.05$ ; Figure 1C and 1D). Subgroup analysis of TMAO with AAA showed that elevated TMAO levels were significantly associated with increased odds of AAA in men but not women, with no statistical significance in the association of TMAO with AAA between men and women (eg, unadjusted quartile

**Table 1. Baseline Characteristics of Participants Stratified by AAA Status in the European AAA Case/Control Cohort (N=352)**

Characteristics	All participants (N=352)	Participants without AAA (n=183)	Participants with AAA (n=169)	P value
Age, mean±SD, y	68.4±5.4	67.2±3.2	69.7±6.8	<0.001
Male sex, n (%)	326 (92.6)	177 (96.7)	149 (88.2)	<0.01
Current smoking, n (%)	80 (22.9)	30 (16.6)	50 (29.8)	<0.01
Hypertension, n (%)	202 (58.0)	91 (50.8)	111 (65.7)	<0.01
Diabetes, n (%)	51 (14.6)	26 (14.4)	25 (14.9)	0.99
CVD, n (%)	40 (11.5)	11 (6.1)	29 (17.3)	<0.01
Renal insufficiency, n (%)	12 (3.4)	3 (1.7)	9 (5.3)	0.078
Statins, n (%)	138 (39.5)	61 (33.3)	77 (46.4)	0.017
Aspirin, n (%)	125 (35.8)	41 (22.4)	84 (50.6)	<0.001
Baseline TMAO, median (IQR), $\mu\text{mol/L}$	4.70 (3.00–8.03)	3.60 (2.50–5.10)	7.40 (4.10–13.80)	<0.001

AAA indicates abdominal aortic aneurysm; CVD, cardiovascular disease; IQR, interquartile range; and TMAO, trimethylamine N-oxide.

AAA defined as a baseline abdominal aortic diameter of  $\geq 3.0$  cm.

The Wilcoxon rank-sum test or Welch 2-sample *t* test for continuous variables and the  $\chi^2$  test or Fisher exact test for categorical variables were used to determine significant differences between groups.

4 versus 1; *P* interaction for men versus women=0.51; Figure S1). Collectively, these data demonstrated that circulating TMAO is associated with AAA in humans.

### Dietary Choline Supplementation Raises TMAO and Augments AAA in a Gut Microbiota-Dependent Manner in Mice

To examine the potential of the meta-organismal TMAO pathway in aneurysm formation, we first used the AngII mouse model of AAA.<sup>28,29</sup> To suppress intestinal microbiota, a cocktail of poorly absorbed broad-spectrum antibiotics (ABX) was administered in the water ad libitum for 1 week before and throughout the study in select mice compared with untreated water. Dietary choline markedly augmented plasma levels of the gut microbial metabolites trimethylamine and TMAO, whereas gut microbiota suppression through ABX diminished plasma trimethylamine and TMAO levels; however, no effect on circulating choline concentrations was observed (Figure S2A–S2C). Conversely, total plasma cholesterol was increased in mice given ABX (Figure S2D). Supplemental dietary choline increased AngII-induced abdominal aortic diameter and aneurysm incidence (increase of  $\geq 50\%$  of baseline or  $\geq 1.2$  mm) compared with mice fed a control diet, whereas ABX suppression of TMAO production eliminated choline-induced increases in these parameters (Figure 2A–2C). Moreover, linear regression analysis using dummy variables to isolate individual treatment effects demonstrated that ABX significantly decreased aortic diameter, and supplemental trimethylamine or TMAO resulted in a significant increase (Table S5). In addition, there was a trend toward increased rupture-induced death in mice fed dietary choline compared

with control-fed and fluoromethylcholine-treated mice (Figure 2D). Notably, dietary choline supplementation (and TMAO elevation) also resulted in more robust thrombus formation and increased macrophage infiltration; moreover, all of these changes were significantly reduced by ABX treatment (Figure 2E–2G). An important finding was that ABX-induced suppression of plasma trimethylamine and TMAO levels, aneurysm diameter, incidence, and rupture were completely reversed by add-back experiments in which mice were concomitantly placed on ABX to suppress gut microbiota and provided either trimethylamine (100 mmol/L) or TMAO (75 mmol/L) in the drinking water, bypassing either the gut microbiota or the entire meta-organismal TMAO pathway (Figure 2A–2D). Although the choline diet increased plasma trimethylamine and TMAO in female mice, AAA diameter and incidence were not significantly different in AngII-infused female mice (Figure S3). Together, these results suggested a direct role for gut microbiome-derived trimethylamine/TMAO in the development of AngII-induced AAA.

### Small-Molecule Inhibition of Gut Microbial Trimethylamine Lyase Activity Decreases Circulating TMAO and Attenuates AAA in Mice

The glycy radical enzyme CutC and its activating protein CutD function together as the primary choline trimethylamine lyase responsible for the conversion of choline to trimethylamine in gut microbes.<sup>30,31</sup> Unlike broad-spectrum ABX, recently developed nonlethal (microbe-friendly) trimethylamine lyase inhibitors were able to significantly decrease plasma TMAO levels in choline-fed mice without affecting other host systems.<sup>17</sup> Mice were provided either the trimethylamine lyase inhibitor



**Table 2. Baseline Characteristics of Participants Stratified by AAA Status in the US AAA Case/Control Cohort (N=1777)**

Characteristics	All participants (N=1777)	Participants without AAA (n=1592)	Participants with AAA (n=185)	P value
Age, mean±SD, y	64.7±11.5	63.9±11.5	71.1±9.1	<0.001
Male sex, n (%)	1185 (66.7)	1037 (65.1)	148 (80.0)	<0.001
Current smoking, n (%)	225 (12.9)	176 (11.3)	49 (26.5)	<0.001
Hypertension, n (%)	1254 (73.1)	1093 (71.4)	161 (87.0)	<0.001
Diabetes, n (%)	578 (32.6)	526 (33.1)	52 (28.1)	0.2
HDL, median(IQR), mg/dL	35.3 (28.5-43.9)	34.9 (28.2-42.6)	45.0 (36.0-53.0)	<0.001
LDL, median(IQR), mg/dL	92.0 (74.0-113.0)	92.0 (75.0-112.0)	85.5 (69.0-125.8)	0.37
CAD, n (%)	1277 (73.3)	1153 (74.1)	124 (67.4)	0.049
CKD, n (%)	336 (19.4)	281 (18.1)	55 (29.7)	<0.001
CRP, median (IQR), mg/L	2.44 (1.08-6.25)	2.37 (1.06-6.19)	3.10 (1.53-6.98)	0.048
Statins, n (%)	1100 (62.0)	961 (60.5)	139 (75.1)	<0.001
Aspirin, n (%)	1180 (66.4)	1055 (66.3)	125 (67.6)	0.79
Baseline TMAO, median (IQR), μmol/L	4.41(2.70-7.24)	4.31(2.63-7.01)	5.22(3.26-9.17)	<0.001

AAA indicates abdominal aortic aneurysm; CAD, coronary artery disease; CKD, chronic kidney disease; CRP, C-reactive protein; HDL, high-density lipoprotein; IQR, interquartile range; LDL, low-density lipoprotein; and TMAO, trimethylamine N-oxide.

AAA was defined as a baseline abdominal aortic diameter of ≥3.0 cm.

The Wilcoxon rank-sum test or Welch 2-sample *t* test for continuous variables and the  $\chi^2$  test for categorical variables were used to determine significant differences between groups.

fluoromethylcholine (0.06 g/L, 0.006% w/t) or regular water ad libitum 1 week before being fed either a choline-enriched or control diet. Mice receiving fluoromethylcholine had drastically reduced levels of circulating plasma trimethylamine and TMAO (Figure S4A and S4B). In addition, provision of fluoromethylcholine significantly reduced choline-augmented aortic dilation, aneurysm incidence, and rupture-induced death compared with placebo (Figure 3A–3C and Table S6). Aortas of mice treated with fluoromethylcholine had significant increases in type I collagen (Figure 3D and Figure S4E) and attenuated accumulation of macrophage infiltration compared with placebo-treated mice (Figure 3D and Figure S4F). A causal role for TMAO in the pathology was further supported by the observation that fluoromethylcholine-induced suppression of plasma TMAO levels, aneurysm diameter, incidence, and rupture were each completely restored by the provision of supplemental TMAO (75 mmol/L) in the drinking water (Figure 3A–3D and Figure S4A–S4D).

To further assess the potential translation value of these findings, we examined the role of choline supplementation and fluoromethylcholine inhibition in an alternative experimental mouse model of AAA. Male C57BL/6J mice (8–10 weeks) were given fluoromethylcholine/water or plain water, as described previously, and underwent the topical elastase model of aneurysm. Similar to the AngII model, supplementation with choline augmented plasma trimethylamine and TMAO, as well as aortic diameters, in the topical elastase model; moreover, all AAA-related phenotypes were completely suppressed by the addition of fluoromethylcholine to

the water (Figure S5). Together, these data support our hypothesis that gut microbe-derived TMAO directly promotes AAA in vivo (≥2 distinct murine models) and that selectively targeting and inhibiting gut microbial trimethylamine lyase activity effectively protects against TMAO generation and AAA formation in mice.

We next examined the gut microbiome in this critical fluoromethylcholine treatment study to determine potential differences in microbial taxa among the groups. We noted that differences in diet, AngII infusion, fluoromethylcholine treatment, and TMAO supplementation can contribute to significant differences in cecal microbiome communities, demonstrating the sensitivity of this unique system (Figure 3E). Principal component analysis of microbial taxa revealed distinct clusters in each independent group, with emphasis on the choline+AngII group to the choline+AngII+fluoromethylcholine group demonstrating the largest shift in microbial taxa (Figure 3F). Analysis of relative microbial taxa abundances showed that choline feeding in the AngII model was associated with enhanced *Parabacteroides* compared with the control diet, which is suppressed by fluoromethylcholine treatment (ie, fluoromethylcholine reversed many supplemental choline diet-induced changes; Figure 3G and 3H). In addition, fluoromethylcholine treatment (versus choline diet alone) was associated with significant enrichment in the genus *Ligilactobacillus* and *Staphylococcus*. In general, these data show that AngII infusion with choline supplementation promotes the reorganization of gut microbial communities, with choline-supplemented diet-induced changes partially reversed by fluoromethylcholine treatment.

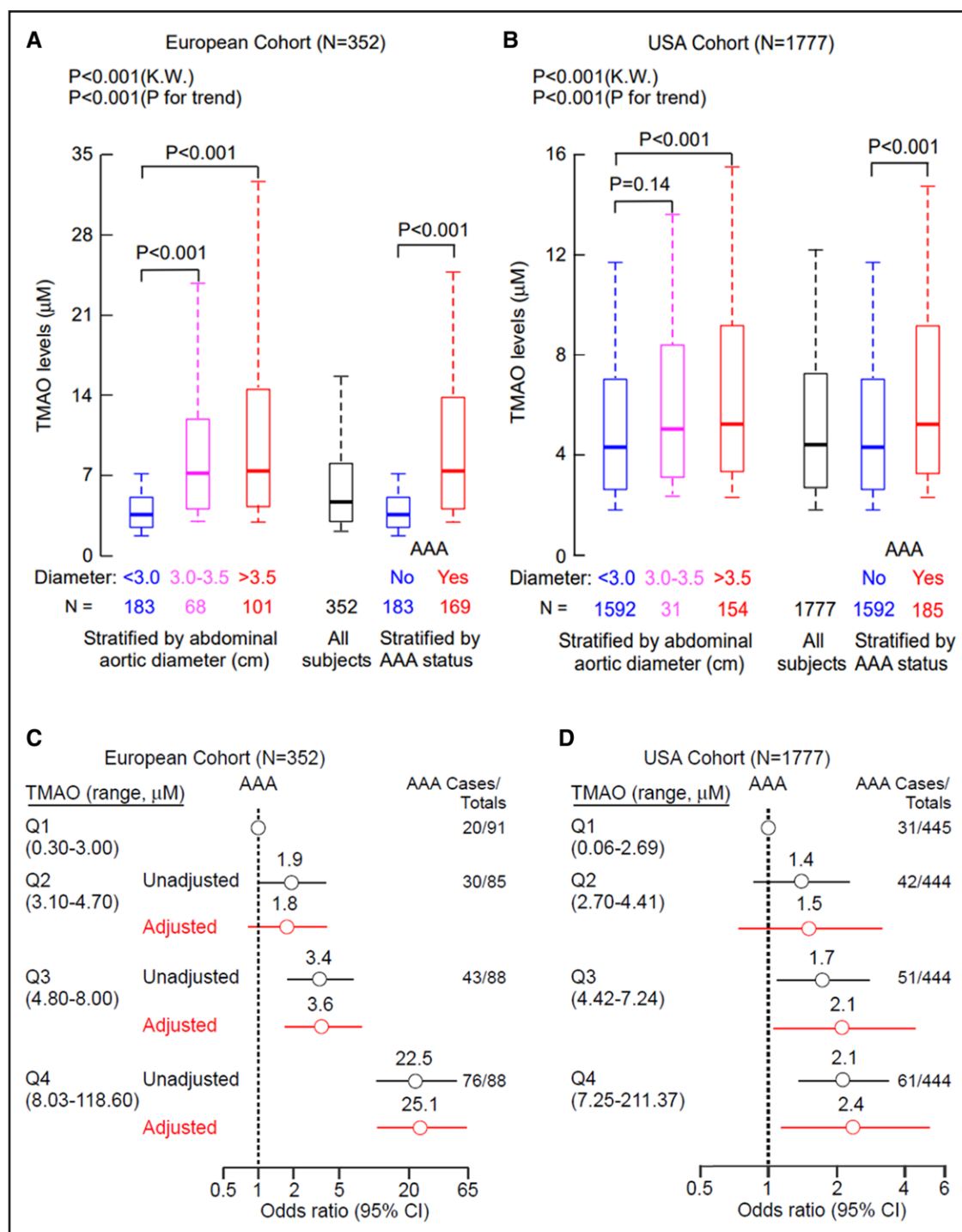


**Figure 1. Association of TMAO levels with AAA in the European and US AAA case-control cohorts.**

Box-whisker plots of trimethylamine N-oxide (TMAO) levels stratified by baseline abdominal aortic diameter and abdominal aortic aneurysm (AAA) status (**A** and **B**). Data are represented as box plots: the middle line is the median; the bottom and top boundaries of the boxes represent the 25th and 75th percentiles; and the whiskers represent the 10th and 90th percentiles.  $P$  values were calculated with Kruskal-Wallis (K.W.) test with a Dunn post hoc analysis, Jonckheere-Terpstra test of increasing trend, and Wilcoxon rank-sum test. Forest plots indicate the odds of AAA according to the quartiles (Qs) of TMAO levels; multivariable logistic regression model for odds ratio included adjustments for age, sex, current smoking, hypertension, diabetes mellitus, cardiovascular disease, statins, aspirin, and renal insufficiency in the European cohort (**C**) and for age, sex, high- and low-density lipoproteins, current smoking, hypertension, diabetes, coronary artery disease, C-reactive protein, statins, aspirin, and chronic kidney disease in the US cohort (**D**). Symbols represent odds ratios, and the 95% CI is indicated by line length. Number of AAA cases and total number of participants in each quartile were included.

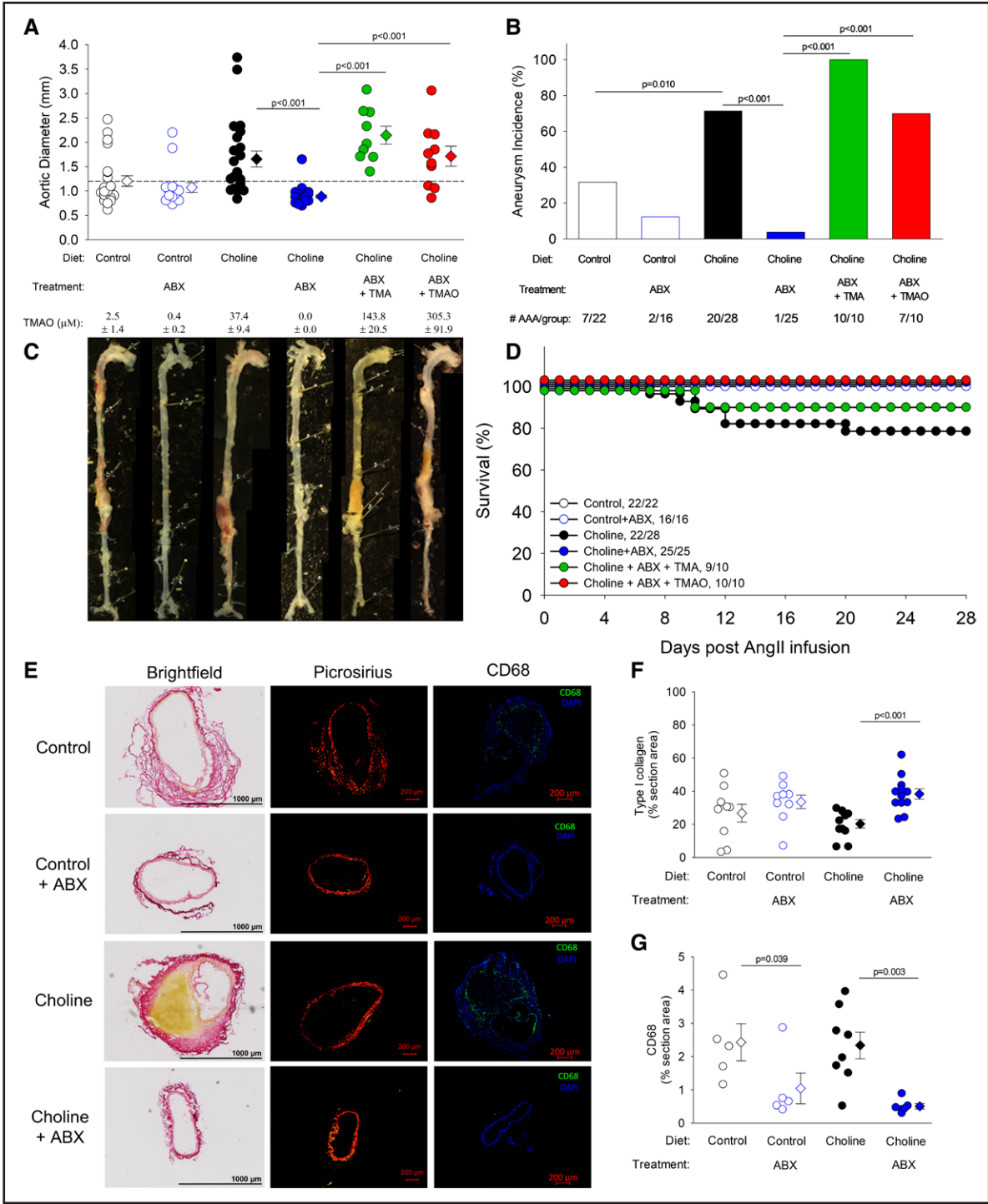


**Figure 2. Dietary choline increases plasma TMAO and augments AAA formation in a gut microbiota/TMAO-dependent manner.** **A**, Aortic diameters from mice fed the indicated diets+poorly absorbed broad-spectrum antibiotics (ABX) and trimethylamine (TMA)/trimethylamine N-oxide (TMAO) supplemented in the drinking water measured ex vivo 28 days after angiotensin II (AngII) infusion (n=10–28 per group). Plasma TMAO levels are displayed as mean $\pm$ SEM for each group (n=9–16 per group). Significance was determined with a Kruskal-Wallis test and Dunn post hoc analysis. **B**, Abdominal aortic aneurysm (AAA) incidence in mice from all groups with an aneurysm defined as an aortic diameter  $\geq$ 1.2 mm or rupture. Total number of aneurysms observed in each group is reported underneath. Significance was determined by multiple pairwise Fisher exact tests. **C**, Representative images of aortas ex vivo from the indicated groups after 28 days of AngII infusion. **D**, Kaplan-Meier curve representing survival and aortic rupture-induced deaths after AngII infusion. Significance was determined by log-rank test. **E**, Representative aortic sections from the indicated groups stained with Picrosirius Red for type I and type III collagen imaged by brightfield (left) and polarized light (middle). Representative aortic sections stained for CD68 (right) and imaged by fluorescent microscopy. **F**, Quantification as percentage of total section area of type I collagen in Picrosirius Red-stained sections and visualized under polarized light (n=9–12 per group). Significance was determined by 2-way ANOVA. **G**, Quantification as percentage of total section area of CD68 (n=5–10 per group). Significance was determined by 2-way ANOVA. Data are represented as data points and mean $\pm$ SEM.

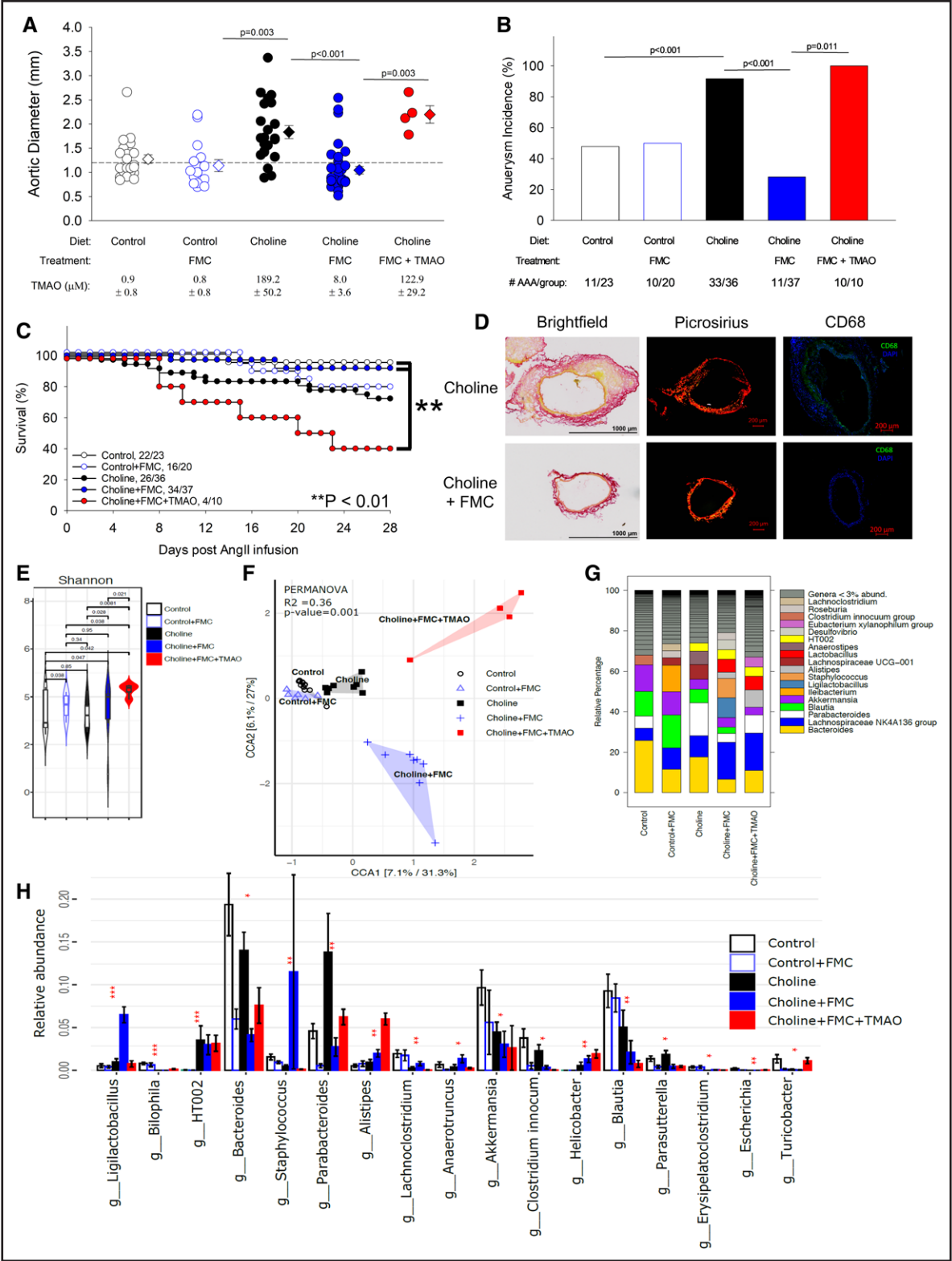


**Figure 3. FMC inhibits gut microbial production of trimethylamine and TMAO from dietary choline and attenuates AAA in choline-fed mice.** **A**, Abdominal aortic diameters from mice fed the indicated diets±fluoromethylcholine (FMC) and trimethylamine N-oxide (TMAO) supplemented in the drinking water measured ex vivo 28 days after angiotensin II (AngII) infusion represented individual data points and mean±SEM (n=4–36 per group). Plasma TMAO levels are shown as mean±SEM for each group (n=4–16 per group). Significance was determined with a Kruskal-Wallis test and Dunn post hoc analysis. **B**, Abdominal aortic aneurysm (AAA) incidence in mice from all groups, with aneurysm defined as abdominal aortic diameter ≥1.2 mm or rupture. Total number of aneurysms observed in each group is reported underneath. (Continued)



**Figure 3 Continued.** Significance was determined by multiple pairwise Fisher exact tests. **C**, Kaplan-Meier curve representing survival and aortic rupture-induced deaths after AngII infusion. Significance was determined by log-rank test. **D**, Representative aortic sections from the indicated groups stained with Picrosirius Red for type I and type III collagen imaged by brightfield (**left**) and polarized light (**middle**). Representative aortic sections stained for CD68 (**right**) and imaged by fluorescent microscopy. **E**, Alpha diversity (Shannon Index) analysis and principal component analysis (**F**) comparing the 5 groups in bacterial diversity of fecal 16S rRNA profiles (n=6–15 per group). **G**, Stacked bar chart representing genera-level relative abundance of the 5 groups (n=6–15 per group). **H**, Bar graph of relative abundance patterns for differentially abundant taxa (random forest;  $P<0.05$ ) representative of genera-level taxa of the 5 groups (n=6–15 per group).

## The Microbial Enzyme Inhibitor Fluoromethylcholine Blocks Progression and Rupture of Established AAA in Mice

Despite decades of progress in therapy and pharmacological interventions for cardiovascular disease, there is still no viable pharmacological approach to limit AAA growth and progression. Given the effectiveness of fluoromethylcholine to prevent AAA formation described previously, fluoromethylcholine was next given to mice with established AAA to determine its potential as a possible interventional therapeutic. *Ldlr*<sup>-/-</sup> mice (n=25) were fed a choline-enriched cholesterol diet for 1 week before and throughout AngII infusion for 42 days. At day 28, mice were stratified into 2 groups with equivalent aneurysmal aortic diameters (aorta >1.2 mm), with 1 group receiving untreated control drinking water (n=9) and the other receiving drinking water supplemented with fluoromethylcholine (0.06 g/L, 0.006% w/t, n=9) for an additional 14 days (Figure 4A). Time-dependent increases in the aortic diameter were significantly blunted in choline-fed/fluoromethylcholine-treated mice versus controls at day 42 (Figure 4B and 4C). In addition, rupture-induced mortality was attenuated with fluoromethylcholine treatment ( $P=0.065$ ; Figure 4D). Plasma trimethylamine/TMAO levels were dramatically reduced (Figure 4E and 4F) at day 42 in mice receiving fluoromethylcholine, whereas plasma choline levels were unaffected (Figure 4G). These data demonstrate the remarkable finding that fluoromethylcholine virtually eliminates TMAO levels and confers protection against growth and rupture of established AAA in mice. Furthermore, this work suggests that using a small-molecule inhibitor to selectively inhibit a gut microbial enzyme (CutC-catalyzed choline trimethylamine lyase activity) may serve as a therapeutic option to prevent the progression and rupture of AAA in patients with newly diagnosed AAA.

## Depletion of Flavin Monooxygenase 3 Activity Reduces Plasma TMAO and Blunts AAA Formation in Mice

After production in the gut flora, trimethylamine is taken up to the portal circulation and transported to the liver, where it is converted to TMAO by hepatic flavin monooxygenases (FMOs), predominantly FMO3.<sup>32</sup> To target the host side of the meta-organismal pathway leading to the production of TMAO, mice genetically deficient in FMO3 were obtained and crossed to the *Ldlr*<sup>-/-</sup> background.<sup>33</sup> As expected, *Ldlr*<sup>-/-</sup>/*Fmo3*<sup>-/-</sup> mice fed a choline diet had sig-

nificantly increased plasma trimethylamine (Figure S6A), whereas plasma TMAO concentrations were significantly decreased (Figure S6B) and plasma choline was unaffected (Figure S6C). AngII-infused *Fmo3*-deficient mice had significantly reduced aortic diameter, AAA incidence, and rupture-induced death compared with proficient controls (Figure 5A–5C). Additional characterization of AAA pathology by either Picrosirius Red or CD68 revealed significantly more type I collagen (Figure 5E) and attenuated macrophage accumulation (Figure 5F), respectively, in *Fmo3*<sup>-/-</sup> mice compared with controls.

As a second approach to inhibit FMO3 production of TMAO, high-choline and cholesterol-rich diet was additionally supplemented with 3,3'-diindolylmethane, a reported inhibitor of FMOs,<sup>34</sup> or cellulose filler as a placebo control. Similar to *Fmo3*<sup>-/-</sup> mice, provision of 3,3'-diindolylmethane significantly increased plasma trimethylamine levels (Figure S6E), whereas plasma TMAO levels were significantly diminished (Figure S6F). Likewise, mice infused with AngII and fed the 3,3'-diindolylmethane-supplemented diet also exhibited reduced aortic diameter (Figure 5G) and AAA incidence (Figure 5H) compared with control-fed mice.

## Dietary Choline Leads to an Upregulation of Genes Associated With ER Stress and Apoptosis

VSMCs undergo significant phenotypic changes in AAA pathology and are critically important to both the initiation and progression of aneurysms.<sup>35</sup> To explore the underlying mechanisms by which TMAO may contribute to AAA, we assessed the effect of TMAO on human aortic VSMCs (HAVSMCs). HAVSMCs were treated with TMAO (100  $\mu$ mol/L) or placebo control (saline) for 5 hours, and next-generation RNA sequencing was performed. The TMAO and saline groups demonstrated spatial separation through principal component analysis (Figure 6A) and heat map clustering (Figure 6B). We identified 792 differentially expressed genes, including 497 upregulated and 295 downregulated differentially expressed genes (Figure 6C). Gene ontology analysis revealed that differentially expressed genes in TMAO-treated HAVSMCs were enriched in response to ER stress and PERK (protein kinase R-like ER kinase)-mediated unfolded protein response (UPR; Figure 6C and Figure S7A). Specifically, PERK, ATF4, ATF5, CHOP (C/EBP homologous protein; also known as DDIT3), GADD34 (growth arrest and DNA damage-inducible

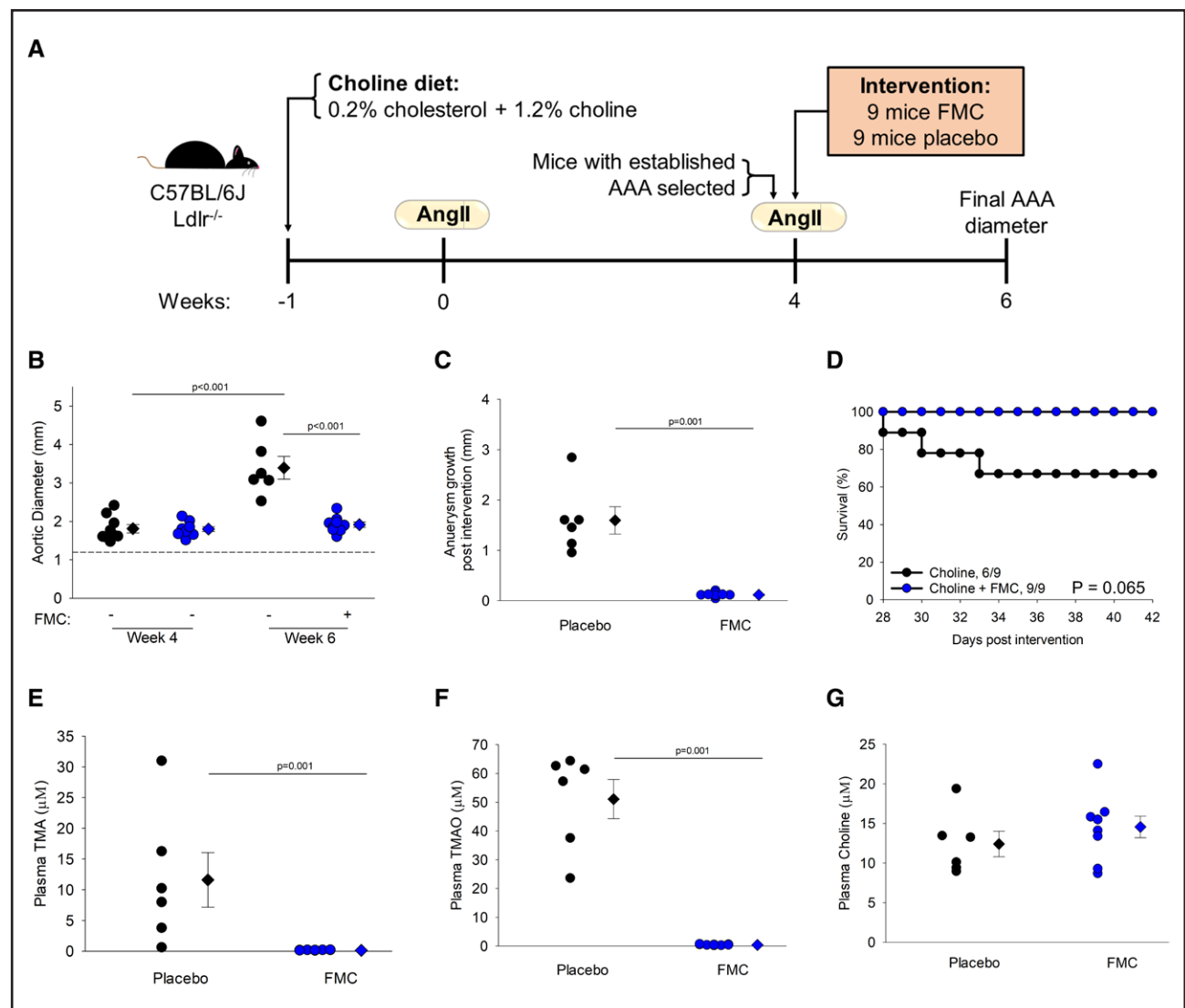


**Figure 4. FMC is protective against growth and rupture of established AAAs in choline-fed mice.**

**A**, Study schematic. Mice were started on choline diet 1 week before initial angiotensin II (AngII) infusion. After 4 weeks, ultrasound was performed to identify mice with developed abdominal aortic aneurysms (AAAs; aortic diameter >1.2 mm). Mice were then randomly assigned to either the fluoromethylcholine (FMC) or placebo treatment groups and subsequently underwent a second round of AngII infusion. Final aortic diameters were measured 2 weeks after the second round of AngII infusion. **B**, Abdominal aortic diameter of mice with established AAA receiving choline diet (n=9) or choline diet+FMC (n=9) at 28 and 42 days. Significance was determined by 2-way ANOVA. **C**, Aneurysm growth as determined by 28- and 42-day ultrasound. Significance was determined by Mann-Whitney rank-sum test. **D**, Kaplan-Meier curve representing survival and rupture-induced deaths after randomization. Significance was tested by log-rank test. Plasma trimethylamine (TMA; **E**), trimethylamine N-oxide (TMAO; **F**), and choline (**G**) measured at end of study by mass spectrometry in the indicated intervention groups (n=6–9 per group). Significance was determined by Student *t* test. Data are represented as data points and mean±SEM.

protein; also known as PPP1R15A), and TRIB3 were markedly upregulated with TMAO treatment (Figure 6D). Because these pathways are most associated with cellular apoptosis, we examined the effects of TMAO-treated HAVSMCs on programmed cell death. Here, we demonstrate that TMAO treatment results in augmented total and cleaved caspase 3, as well as significantly reduced cell viability with augmented early and late apoptosis in HAVSMCs (Figure 6E–6H). In addition, protein levels of matrix and active matrix metalloproteinase-2 were significantly increased in aortic

VSMCs treated with TMAO compared with vehicle control (Figure S7B and S7C).

To verify that these effects occurred in vivo, male *Ldlr*<sup>-/-</sup> mice were fed either a low-choline and cholesterol-rich diet (control) or a high-choline cholesterol-rich diet for 1 week, infused with AngII for 3 days, and euthanized; aortas were collected and RNA sequencing was performed on the suprarenal abdominal aorta (Figure 7A). Similar to HAVSMCs, choline feeding, in combination with AngII, augmented genes associated with apoptosis, ER stress, and the UPR (Figure 7B). Among

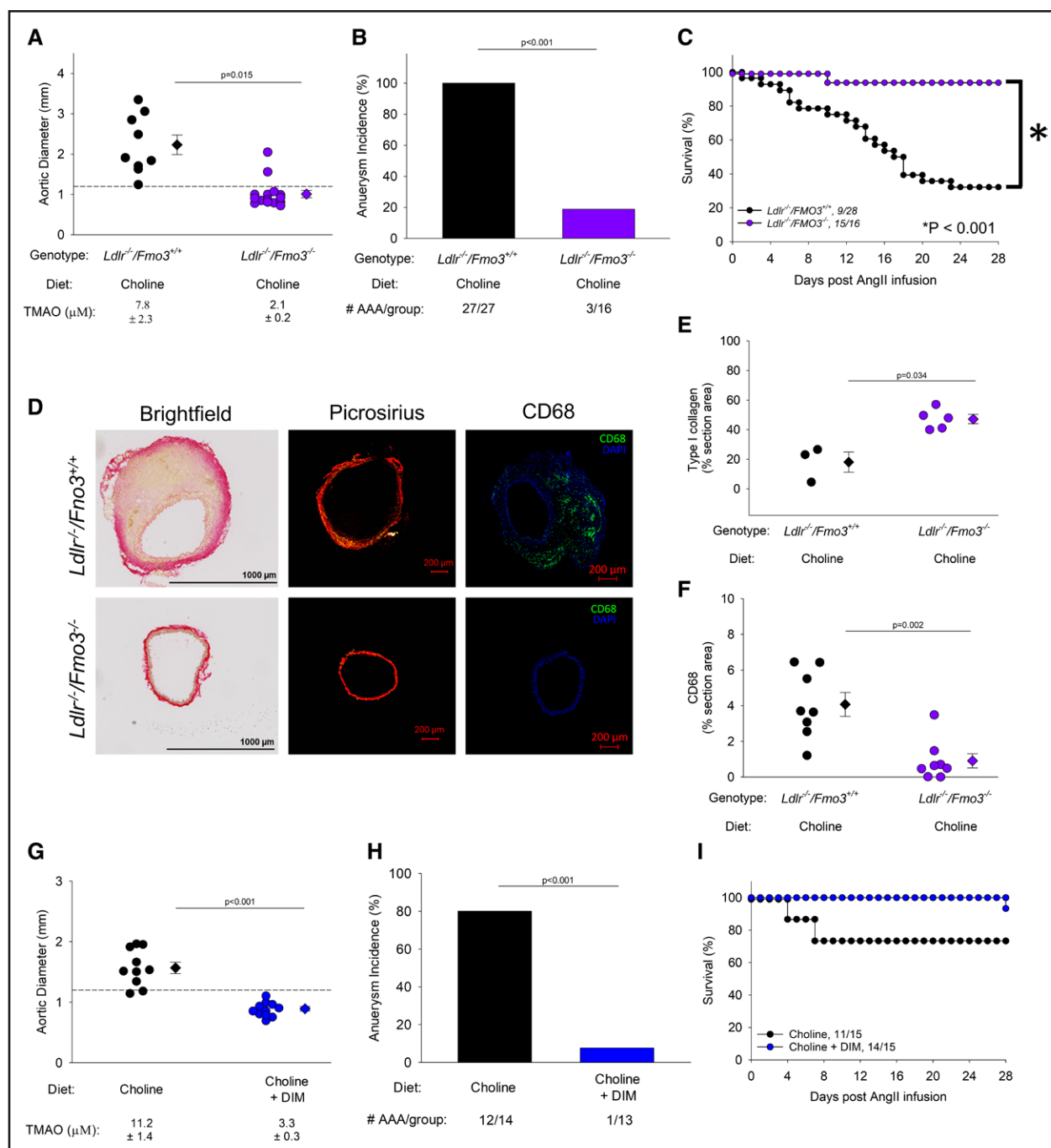


**Figure 5. Disruption of FMO3 production of TMAO protects mice from AngII-induced AAA.**

**A**, Aortic diameters in *Ldlr*<sup>-/-</sup>/*Fmo3*<sup>-/-</sup> vs *Ldlr*<sup>-/-</sup>/*Fmo3*<sup>+/+</sup> mice measured ex vivo 28 days after angiotensin II (AngII) infusion (n=9–15 per group). Plasma trimethylamine N-oxide (TMAO) levels are displayed as mean±SEM for each group (n=8 per group). Significance was determined by Student *t* test. **B**, Abdominal aortic aneurysm (AAA) incidence with an aneurysm defined as aortic diameter ≥1.2 mm or rupture. Total number of aneurysms observed in each group is reported underneath. Significance was determined by multiple pairwise Fisher exact tests. **C**, Kaplan-Meier curve representing survival and aortic rupture-induced deaths after AngII infusion. Significance was determined by log-rank test. **D**, Representative aortic sections from the indicated genotypes stained with Picrosirius Red for type I and type III collagen imaged by brightfield (left) and polarized light (middle). Representative aortic sections were stained for CD68 (right) and imaged by fluorescent microscopy. **E**, Quantification as percentage of total section area of type I collagen in Picrosirius Red-stained sections and visualized under polarized light. Significance was determined by Student *t* test (n=3–5 per group). **F**, Quantification of CD68 staining as percentage of total section area of CD68 positive (n=8 per group). Significance was determined by Student *t* test. **G**, Aortic diameters measured ex vivo 28 days after AngII infusion from mice given dietary 3,3'-diindolylmethane (DIM) compared with placebo treatment (n=10–12 per group). Plasma TMAO levels are displayed as mean±SEM for each group (n=10–14 per group). Significance was determined by Student *t* test. **H**, AAA incidence with an aneurysm defined as aortic diameter ≥1.2 mm or rupture. Total number of aneurysms observed in each group is reported underneath. Significance was determined by Fisher exact test. **I**, Kaplan-Meier curve representing survival and aortic rupture-induced deaths after AngII infusion. Significance was determined by log-rank test. Data are represented as data points and mean±SEM. FMO3 indicates flavin monooxygenase 3.

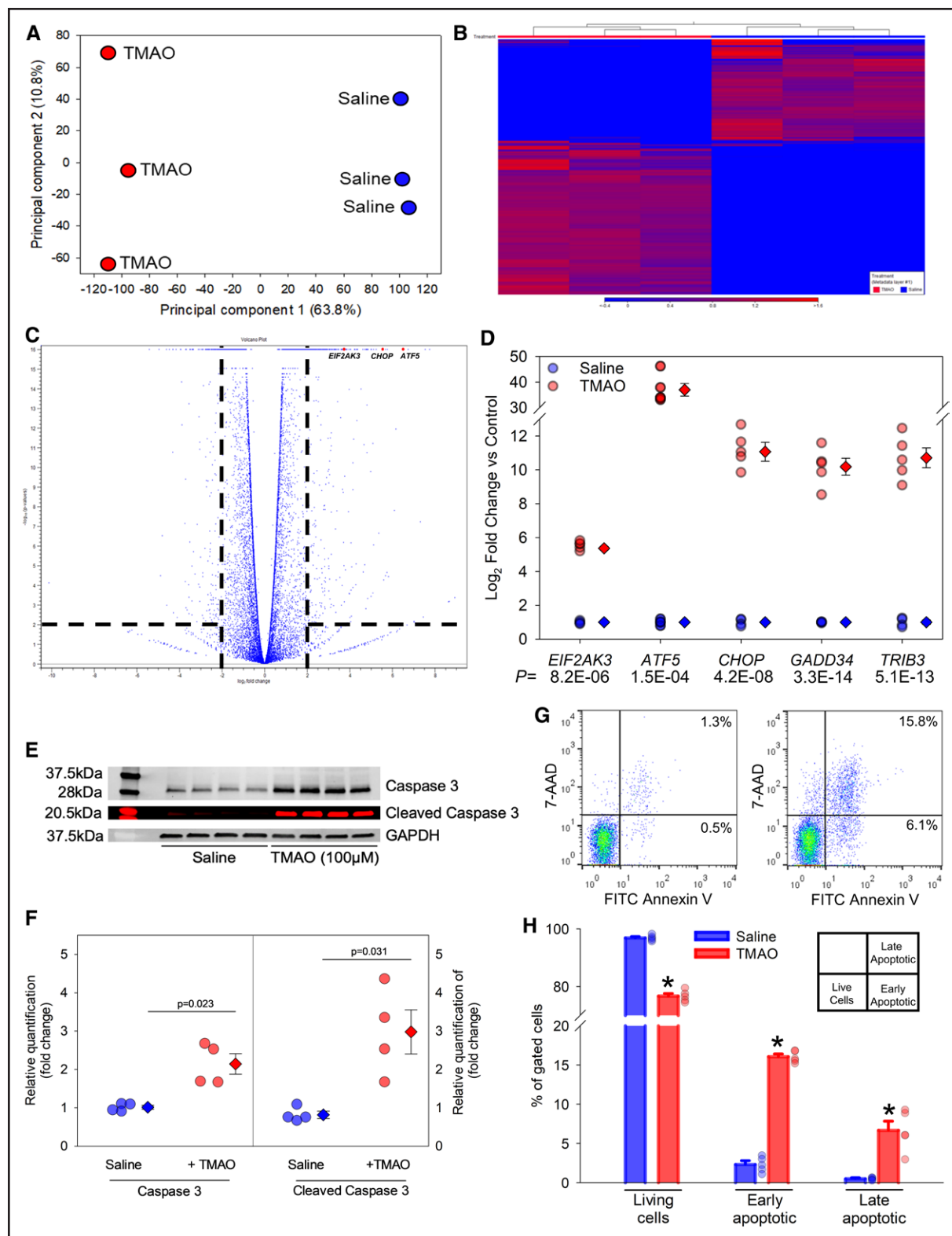


**Figure 6. RNA sequencing demonstrates increased apoptosis and ER stress and decreased autophagy with TMAO treatment in vitro.** Human aortic vascular smooth muscle cells (HAVSMCs) were prepared with 3 independent samples, conducted in triplicate, treated with either sterile saline or trimethylamine N-oxide (TMAO; 100 μmol/L) for 5 hours, after which RNA was processed and RNA sequencing was performed. **A**, Principal component analysis and heat map clustering (**B**) of RNA sequencing data comparing TMAO (100 μmol/L) with saline control. **C**, Volcano plot of differentially expressed genes between TMAO- and saline-treated HAVSMCs and fold change (**D**) of unfolded protein response pathway-related genes. **E**, Representative Western blot and quantification of caspase 3 and activated caspase 3 protein levels in TMAO- and saline-treated HAVSMCs (**F**) saline, n=4; TMAO, n=4). Significance was determined by Student *t* test. **G**, Representative and quantified (**H**) (*Continued*)



**Figure 6 Continued.** results of flow cytometry analyses for apoptotic cells identified by annexin V and 7-aminoactinomycin D using the indicated gating strategy (n=5 per group). Circles represent individual data points; diamonds are mean±SEM. *P* values are listed in figure, or \**P*<0.01. Relative quantification and gated cells were analyzed with a Kruskal-Wallis test and Dunn post hoc analysis. Significance is defined as fold change ≥1.5 and false discovery rate *P*≤0.05 with Cuffdiff. ER indicates endoplasmic reticulum.

the most upregulated genes was *Eif2ak3* (*Perk*), which was increased exponentially over saline chow (256-fold) and AngII chow (120-fold; Figure 7C). Several other genes upregulated in our analysis encode proteins of the *Perk* arm of the UPR, including *Atf4* and *Chop* (Figure 7C). These results were confirmed by quantitative real-time polymerase chain reaction for *Perk* and *Atf4* (Figure S7D and S7E). Caspase 3 (*Casp3*), a cysteine protease that plays an essential role in apoptosis, was also significantly upregulated in the aortas of choline-fed mice. Atg5 (autophagy-related 5) and Becn1 (beclin 1), 2 autophagy-related proteins, were among the genes most significantly downregulated in the aortas of choline-fed mice (Figure 6B).

Recent studies report that TMAO binds to PERK and selectively activates the PERK branch of the UPR.<sup>34</sup> Our data demonstrate that TMAO treatment of HAVSMCs and a high-choline diet also augment PERK. To determine whether choline-induced increases in apoptosis and UPR are attributable to PERK, we repeated our analysis of the aortic transcriptome with the addition of a PERK inhibitor fed concomitantly with the high-choline and cholesterol-rich diet and during AngII infusion (Figure 7A). Inhibition of PERK resulted in a complete ablation of choline-induced UPR activation and caspase-induced genes (Figure 7C). PERK inhibition reversed effects seen with autophagy, resulting in augmented levels of Atg5 and Becn1. Principal component analysis demonstrated that PERK inhibition shifts the gene clusters toward control chow-fed mice (Figure 7D). In contrast to a previous study suggesting that TMAO-induced aneurysm formation was attributable to upregulated VSMC senescence, we found that senescent genes *CDKN1A* (p21), *CDKN2C* (p14/p16), and *GLB* (β-galactosidase) were decreased in our human VSMCs treated with TMAO (Figure S8A) and our in vivo model (Figure S8B).<sup>36</sup> Overall, these data confirm a relationship between TMAO and PERK-mediated UPR and, together with our in vivo data, suggest that TMAO mechanistically contributes to AAA through activation of PERK-mediated UPR and VSMC apoptosis.

## DISCUSSION

Despite significant advancements in pharmacological treatments of other cardiovascular diseases, no effective druggable targets have been identified as effective in reducing AAA; rather, the preferred treatment remains surgical repair.<sup>1,2,37</sup> Several placebo-controlled studies aimed at potential pharmacological therapies to treat AAA, including the use of statins, angiotensin-converting enzyme II inhibitors, and antiplatelet

agents, have failed to show a decrease in AAA burden, highlighting the need for novel therapeutic targets.<sup>37</sup> Our studies indicate that targeting of the gut microbial TMAO pathway reduces aneurysm severity and mortality in vivo. We demonstrate that ABX proved to be an effective way to suppress microbiome-derived TMAO aneurysm formation in the AngII mouse model. However, ABX treatment alone also modestly inhibited aortic diameter increases in our model. This may be attributable to broad-spectrum matrix metalloproteinase inhibition, which has been demonstrated most prominently with doxycycline.<sup>38</sup> Although our studies demonstrate that this effect can be reversed with exogenous TMAO supplementation, highlighting the importance of TMAO, the overall use of ABX does not represent a viable therapeutic option in patients with an aneurysm. Human trials administering doxycycline to patients with AAA have been largely unsuccessful in reducing aneurysm growth.<sup>39</sup> This may be a result of ABX creating a negative selection pressure on gut microbes, leading to unpredictable changes in the microbial taxa, development of ABX resistance, overgrowth of opportunistic organisms after cessation of ABX, and ultimately increases in inflammatory profiles and gut dysbiosis.<sup>10</sup> Therefore, we used a suicide substrate inhibitor, fluoromethylcholine, which is nonlethal to microbes and irreversibly modifies the enzymatic dyad CutC/D in microbes expressing this gene cluster.<sup>17</sup> Fluoromethylcholine inhibition of TMAO inhibited choline diet-induced aneurysm formation in 2 distinct mouse models and almost completely blunted aortic diameter growth and death in a model of preexisting AAA disease, halting progression. Fluoromethylcholine treatment was also characterized by reversing some choline-rich diet-induced changes in microbial community structure and induced an increase in species diversity that is generally associated with a healthier microbial community. More important, our work suggests that gut microbial inhibition of TMAO generation may be a potentially safe and novel therapeutic target for the prevention of AAA progression and rupture in humans.

Inflammation has long been recognized as a hallmark of AAA progression.<sup>4</sup> Increased cytokine expression and cell adhesion markers recruit infiltrating immune cells to the vessel wall, which act to further enhance the inflammatory milieu. TMAO has also been intimately linked to inflammation in various cell types. For instance, prolonged choline feeding of hypercholesterolemic *Ldlr*<sup>-/-</sup> mice results in no appreciable changes in lipid and glucose parameters, but markedly elevated choline-induced TMAO is correlated with increased levels of macrophage *Cd68*, *Cox-2*, and *Tnfa* expression in the aorta.<sup>15</sup>

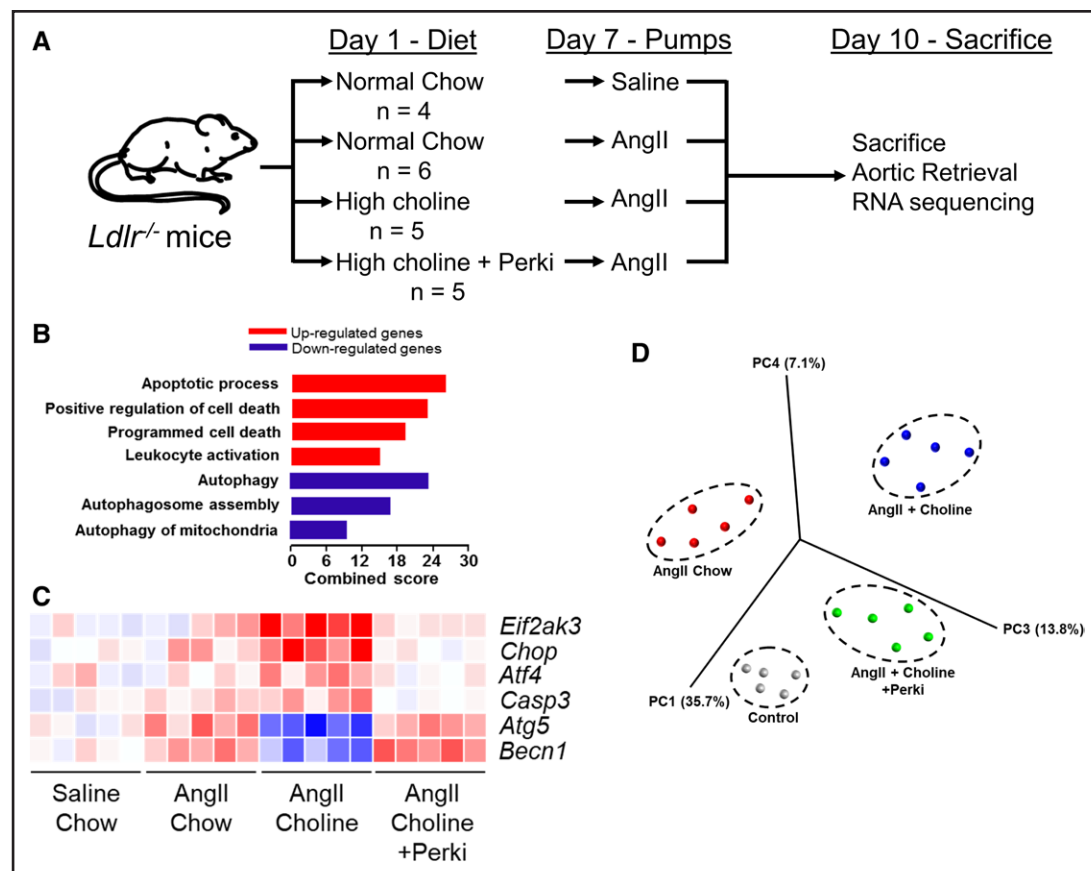


**Figure 7. RNA sequencing demonstrates that short-term choline feeding in the AngII AAA mouse model increased apoptosis and ER stress while decreasing autophagy.**

**A**, Experimental schematic for RNA sequencing analysis from whole abdominal aortic sections from the indicated groups for pathway analysis (**B**) and gene expression changes (**C**) in the abdominal aorta isolated from *Ldlr*<sup>-/-</sup> mice fed a control diet with saline infusion (n=4), control diet with angiotensin II (AngII) infusion (n=6), choline diet with AngII infusion (n=5), or choline diet with AngII infusion plus PERK inhibitor (n=5). **D**, Spatial separation between indicated groups examined with principal component analysis. AAA indicates abdominal aortic aneurysm; and ER, endoplasmic reticulum.

Subsequent treatment of HAVSMCs demonstrates that this TMAO induction is attributable to the activation of p-38 mitogen-activated protein kinase and nuclear factor- $\kappa$ B.<sup>15,40</sup> Here, we demonstrate that choline feeding increases macrophage CD68 infiltration in choline-fed AngII-infused *Ldlr*<sup>-/-</sup> mice and, likewise, that TMAO treatment of HAVSMCs increases *COX2* (4.72-fold increase) and *TNF $\alpha$*  (6.07-fold increase) compared with saline-treated cells (data not shown). It is important to note that increased levels of *COX2* and *TNF $\alpha$*  are also linked to aneurysm formation and progression in several studies.<sup>41,42</sup> Moreover, TMAO has been found to induce both the nucleotide-binding oligomerization domain-like receptor family pyrin domain-containing 3 inflammasome in the aortas of an apolipoprotein E-deficient (*apoE*<sup>-/-</sup>) mouse model through its effectors interleukin-1 $\beta$ , caspase 1, and interleukin-18,<sup>40</sup> where the inflammasome and these mediators are also linked to AAA formation.<sup>43</sup> However, neither our TMAO-treated HAVSMCs nor our choline-fed *Ldlr*<sup>-/-</sup> mice have any increases in *NLRP3*, *IL-1 $\beta$* , *CASP1*, or *IL-18* expression (data not shown).

Although the results of this study indicate a mechanism for TMAO driven through increased PERK-mediated UPR signaling, other known proinflammatory/thrombotic activity of TMAO could also contribute to the worsening of AAAs.

Although AAAs can occur in both sexes, the incidence rate and mortality rate are greater in men.<sup>2,3</sup> Previous studies demonstrate that these effects are most likely attributable to sex hormones, with testosterone being one of the main agonists of aneurysm severity and ultimate mortality.<sup>44,45</sup> Despite the limitations of mouse models of AAA compared with human pathophysiology, the AngII model has a well-established biology compatible with human AAA ruptures and sex-related differences.<sup>46</sup> Regardless of the profound effect we observe in our studies with the gut microbe-derived TMAO pathway in male mice, we did not observe increases in aneurysm incidence or diameter in choline-fed AngII-infused female mice, even with similarly increased levels of TMAO. Moreover, in the US cohort, 592 women were enrolled, but only 37 cases with AAA were included, putting the overall prevalence of

AAA in our American cohort lower in women (6.3%) than in men (12.5%). Similar to our mouse studies, we found no significant relationship with elevated TMAO and the odds of AAA in women. However, it should be noted that we did not have any female patients in our European cohort, and the overall relationship between TMAO levels and AAA in women warrants further investigation in a larger independent validation study. Although multiple US medical societies have clear age-specific guidelines for screening men with certain risk factors for infrarenal AAA, no such guideline exists for women, and our numbers are therefore reflective of real-life clinical data.<sup>3</sup>

The UPR is a homeostatic monitoring system for protein biosynthesis, which can detect ER stress from unfolded and misfolded proteins, resulting in activation and downstream signaling either to restore ER protein homeostasis or to mitigate apoptosis and cell death.<sup>47</sup> Our data demonstrate that choline diet with AngII infusion results in a marked upregulation of only the PERK-eIF2-ATF4 arm of the UPR signaling pathway, with exponential increases in both PERK (256-fold increase) and ATF4 (15-fold increase). We demonstrate that CHOP is likewise increased (75-fold increase) over AngII infusion alone, suggesting choline-induced TMAO-specific amplification of these pathways. Previous studies have shown that both calcium chloride and AngII induction of aneurysms in mice result in increased UPR signaling, which are similarly upregulated in human AAA specimens.<sup>48,49</sup> Furthermore, a recent study demonstrated that TMAO selectively activates the PERK branch of the UPR at physiologically relevant concentrations.<sup>34</sup> It is important to note that when mice are given a PERK inhibitor, choline- and AngII-induced activation of the PERK arm of the UPR is completely attenuated. We speculated that TMAO was targeting the VSMC region of the aorta because depletion of this cell population is recognized as a key mediator in the degeneration and dilation of the aorta characteristic of AAA formation.<sup>50</sup> Indeed, treatment of HAVSMCs resulted in the similar upregulation of PERK and CHOP found in our in vivo studies. Moreover, one of the highest upregulated genes in TMAO-treated VSMCs was *ATF5* (40-fold increased over saline control), which serves to potentiate CHOP-dependent apoptosis. Similarly, *GADD34* and *TRB3* are also increased 10-fold over control, which represents another proapoptotic mechanism of prolonged CHOP expression by inducing translation recovery and inhibition of the ERK prosurvival pathway, respectively.<sup>51</sup> Alternative to apoptosis, the UPR also regulates autophagy, which is critical for vascular integrity during aneurysms. Although our data show that ER stress and UPR signaling are augmented, the autophagy-related genes *Atg5* and *Becn1* are downregulated with choline supplementation in vivo. Therefore, our data indicate that increased circulating TMAO induces the PERK arm of the UPR, resulting in increased VSMC apoptosis and decreased

autophagy, which results in the augmented progression of AAA. Future studies will examine the mechanistic link of the TMAO-ER stress-UPR-apoptosis-autophagy axis in aneurysm formation and progression.

Several studies have advanced the field of small-molecule nonlethal bacterial enzyme inhibitors as a novel therapeutic option to affect the microbial production of inflammatory mediators such as TMAO. Specifically, the gut microbe-targeted choline trimethylamine lyase inhibitor fluoromethylcholine significantly remodels the cecal microbiome in mice, which reverses choline-induced changes with no evidence of toxicity.<sup>17</sup> Although it is important to note that our analyses were conducted at the genus level, our study demonstrates that the CutC/D microbial taxa *Escherichia* was altered by both choline diet and fluoromethylcholine treatment in our model. The lack of changes in other CutC/D microbial taxa may be attributable in part to the low abundance of these microbes, making detection of specific and meaningful changes difficult to assess.<sup>52</sup> Previous studies by our group of researchers have demonstrated that fecal microbiome composition does not predict dietary production of TMAO, so our lack of changes in CutC/D taxa is not overly concerning. Moreover, the overall changes in the gut microbial endocrine organ are exquisitely sensitive to environmental and dietary factors, so the impact of these newly developed bacterial enzyme inhibitors on the total microbial landscape (not just the CutC/D taxa) is critical to the relationship of microbes with cardiovascular disease outcomes.<sup>53</sup> For instance, fluoromethylcholine treatment significantly decreased the prevalence of *Parabacteroides*, a taxa containing 15 known subspecies that have been implicated as both proinflammatory and anti-inflammatory mediators in mouse models of inflammatory bowel disease.<sup>54</sup> Moreover, we found that the abundance of *Lactobacillus* was significantly increased in choline-fed and fluoromethylcholine-treated mice. Supplemental *Lactobacillus rhamnosus* GR-1 has been used as a probiotic for the treatment of myocardial infarction, resulting in improvement of systolic and diastolic left ventricular function in rodent models.<sup>55</sup> Although the impact of specific gut microbes on AAA progression remains unclear, the link between the gut microbiome and cardiometabolic diseases is evident. It will be beneficial to understand how therapies modify gut microbiome to find optimal druggable targets and to maximize therapeutic potential.

A previous study demonstrated that delivery of TMAO to *apoE*<sup>-/-</sup> mice infused with AngII or C57BL/6J mice exposed to calcium chloride resulted in augmented aneurysm formation, which was attributed to VSMC senescence and reactive oxygen species.<sup>56</sup> TMAO delivery increased the senescent markers p16 and p21 and augmented senescent-associated  $\beta$ -galactosidase expression in both aneurysm models, as well as in ex vivo VSMCs treated with TMAO.<sup>56</sup> Our results are in contrast to this study in that we found no clear association with

senescent programs in either our in vivo mouse model or our ex vivo VSMC cultures through the examination of RNA sequencing. It is possible that this discrepancy may result from the different experimental designs. Previous studies examined advanced aneurysms after 28 days of exogenous TMAO administration for immunohistochemistry and Western blotting; our results were examined at an early time point of 3 days after aneurysm initiation with choline-induced TMAO production and examination by RNA expression. It should be noted that although these effects are confirmed in VSMCs, the majority of the staining appears to be extravascular in the adventitial regions of the aortic tissue. Furthermore, our results confirm previous studies demonstrating that TMAO activates a PERK-mediated pathway of ER stress, which is most often associated with apoptotic signaling.<sup>34</sup> Although apoptosis and senescence are considered 2 of the major outcomes on irreversible cellular damage, these 2 events are not related and have distinctive biological pathways.<sup>57</sup> Moreover, senescent cells are shown to be resistant to apoptosis, which is in contrast to our mechanistic findings and previous literature demonstrating the critical role of apoptosis in aneurysm pathophysiology.<sup>57,58</sup>

## Conclusions

This work demonstrates a relationship between plasma TMAO and AAA in both humans and mice and establishes a causal role for the gut microbiota in AAA disease. It also indicates that TMAO directly participates in AAA pathogenesis, specifically through the activation of the PERK arm of the UPR. Furthermore, this work indicates that the gut microbiota may be selectively targeted to prevent the generation of TMAO and the development, progression, and rupture of AAAs. These findings suggest that selectively targeting the gut microbiota may be a feasible therapeutic option for the treatment of AAA in humans. With treatment options limited for patients with AAA, this work has the potential to drastically shift clinical care and patient outcomes in this disease population.

## ARTICLE INFORMATION

Received April 25, 2022; accepted February 7, 2023.

### Affiliations

Department of Internal Medicine (T.W.B., K.A.C., T.M.C., C.W.-L., S.F., H.M.R., M. Brooks, M.T., A.P.O.), Department of Environmental Health (T.S.), Division of Cardiovascular Health & Disease (T.W.B., K.A.C., T.M.C., C.W.-L., S.F., H.M.R., M. Brooks, M.T., A.P.O.), Division of Biostatistics and Bioinformatics (T.S.), and Pathobiology and Molecular Medicine Graduate Program (K.A.C., T.M.C., C.W.-L., H.M.R., M.T., A.P.O.), University of Cincinnati College of Medicine, OH. Department of Cardiovascular and Metabolic Sciences, Learner Research Institute (X.S.L., Z.W., R.N.H., R.C.S., J.A.B., N.S., R.B., A.A., C.P., W.H.W.T., S.J.C., J.M.B., S.L.H.), Center for Microbiome & Human Health (X.S.L., Z.W., J.A.B., N.S., W.H.W.T., J.M.B., S.L.H.), and Department of Cardiovascular Medicine, Heart, Vascular and Thoracic Institute (R.B., W.H.W.T., S.J.C., S.L.H.), Cleveland Clinic, OH. Section of Vascular Surgery, Department of Surgical Sciences, Uppsala University, Sweden (K.M., M. Björck, A.W.). Division of Endocrinology, Boston Children's Hospital, Harvard Medical School, MA (S.B.).

## Acknowledgments

T.W.B., K.A.C., J.M.B., S.L.H., and A.P.O. conceived and designed the study. T.W.B., K.A.C., H.M.R., T.M.C., C.W.-L., S.F., and M.B. were responsible for animal care. S.J.C., R.N.H., R.N.S., J.A.B., K.M., M.B., A.W., Z.W., J.M.B., S.L.H., and A.P.O. were responsible for phlebotomy, clinical data management, and regulation. A.P.O., T.W.B., K.A.C., X.S.L., R.N.H., R.N.S., and Z.W. conducted laboratory testing. T.W.B., K.A.C., X.S.L., R.N.H., R.N.S., N.S., Z.W., M.T., S.J.C., S.L.H., and A.P.O. contributed to data processing. T.W.B., K.A.C., and A.P.O. supervised all aspects of the study. T.W.B., K.A.C., and A.P.O. contributed to initial data interpretation and wrote the manuscript. All authors contributed to final data interpretation and critical revision of the manuscript and approved the final version of the manuscript.

## Sources of Funding

This work was supported by National Institutes of Health (NIH) grants R01-HL147171 (Dr Owens), R01-HL158801-01 (Dr Cameron), T32 HL125204 (Dr Benson), R01HL103866 (Dr Hazen), and P01HL147823 (Drs Hazen and Brown). Aspects of the project were supported by the National Center for Advancing Translational Sciences of NIH under award 2UL1TR001425.

## Disclosures

Drs Hazen and Wang report being named co-inventors on pending and issued patents held by the Cleveland Clinic relating to cardiovascular diagnostics and therapeutics and being eligible to receive royalty payments for inventions or discoveries related to cardiovascular diagnostics or therapeutics from Cleveland HeartLab, a wholly owned subsidiary of Quest Diagnostics, Procter & Gamble, and Zehna Therapeutics. Dr Hazen reports being a paid consultant for Procter & Gamble and Zehna Therapeutics and having received research funds from Procter & Gamble, Zehna Therapeutics, and Roche Diagnostics. Dr Brown reports being named a co-inventor on pending and issued patents held by the Cleveland Clinic relating to cardiovascular and metabolic disease therapeutics and being eligible to receive royalty payments for inventions or discoveries related to cardiometabolic therapeutics from Zehna Therapeutics. The other authors report no conflicts.

## Supplemental Material

Complete Materials and Methods

Tables S1–S6

Figures S1–S8

Full unedited gels for Figure 7E

References 59–71

## REFERENCES

- Gerhard-Herman MD, Gornik HL, Barrett C, Barshes NR, Corriere MA, Drachman DE, Fleisher LA, Fowkes FGR, Hamburg NM, Kinlay S, et al. 2016 AHA/ACC guideline on the management of patients with lower extremity peripheral artery disease: executive summary: a report of the American College of Cardiology/American Heart Association Task Force on Clinical Practice Guidelines. *J Am Coll Cardiol*. 2017;69:1465–1508. doi: 10.1016/j.jacc.2016.11.008
- Gillum RF. Epidemiology of aortic aneurysm in the United States. *J Clin Epidemiol*. 1995;48:1289–1298. doi: 10.1016/0895-4356(95)00045-3
- Owens DK, Davidson KW, Krist AH, Barry MJ, Cabana M, Caughey AB, Doubeni CA, Epling JW Jr, Kubik M, Landefeld CS, et al; US Preventive Services Task Force. Screening for abdominal aortic aneurysm: US Preventive Services Task Force recommendation statement. *JAMA*. 2019;322:2211–2218. doi: 10.1001/jama.2019.18928
- Kuivaniemi H, Ryer EJ, Elmore JR, Tromp G. Understanding the pathogenesis of abdominal aortic aneurysms. *Expert Rev Cardiovasc Ther*. 2015;13:975–987. doi: 10.1586/14779072.2015.1074861
- Kessler V, Klopff J, Eilenberg W, Neumayer C, Brostjan C. AAA revisited: a comprehensive review of risk factors, management, and hallmarks of pathogenesis. *Biomedicines*. 2022;10:94. doi: 10.3390/biomedicines10010094
- Lindholt JS, Henneberg EW, Juul S, Fasting H. Impaired results of a randomised double blinded clinical trial of propranolol versus placebo on the expansion rate of small abdominal aortic aneurysms. *Int Angiol*. 1999;18:52–57.
- Takagi H, Yamamoto H, Iwata K, Goto S, Umemoto T; ALICE (All-Literature Investigation of Cardiovascular Evidence) Group. Effects of statin therapy on abdominal aortic aneurysm growth: a meta-analysis and meta-regression of observational comparative studies. *Eur J Vasc Endovasc Surg*. 2012;44:287–292. doi: 10.1016/j.ejvs.2012.06.021



8. Sweeting MJ, Thompson SG, Brown LC, Greenhalgh RM, Powell JT. Use of angiotensin converting enzyme inhibitors is associated with increased growth rate of abdominal aortic aneurysms. *J Vasc Surg*. 2010;52:1–4. doi: 10.1016/j.jvs.2010.02.264
9. Kristensen KE, Torp-Pedersen C, Gislason GH, Egfrjord M, Rasmussen HB, Hansen PR. Angiotensin-converting enzyme inhibitors and angiotensin II receptor blockers in patients with abdominal aortic aneurysms: nationwide cohort study. *Arterioscler Thromb Vasc Biol*. 2015;35:733–740. doi: 10.1161/ATVBAHA.114.304428
10. Witkowski M, Weeks TL, Hazen SL. Gut microbiota and cardiovascular disease. *Circ Res*. 2020;127:553–570. doi: 10.1161/CIRCRESAHA.120.316242
11. Brown JM, Hazen SL. Metaorganismal nutrient metabolism as a basis of cardiovascular disease. *Curr Opin Lipidol*. 2014;25:48–53. doi: 10.1097/MOL.0000000000000036
12. Wang Z, Klipfell E, Bennett BJ, Koeth R, Levison BS, Dugar B, Feldstein AE, Britt EB, Fu X, Chung YM, et al. Gut flora metabolism of phosphatidylcholine promotes cardiovascular disease. *Nature*. 2011;472:57–63. doi: 10.1038/nature09922
13. Zhu W, Gregory JC, Org E, Buffa JA, Gupta N, Wang Z, Li L, Fu X, Wu Y, Mehrabian M, et al. Gut microbial metabolite TMAO enhances platelet hyperreactivity and thrombosis risk. *Cell*. 2016;165:111–124. doi: 10.1016/j.cell.2016.02.011
14. Zhu W, Romano KA, Li L, Buffa JA, Sangwan N, Prakash P, Tittle AN, Li XS, Fu X, Androjna C, et al. Gut microbes impact stroke severity via the trimethylamine N-oxide pathway. *Cell Host Microbe*. 2021;29:1199–1208.e5. doi: 10.1016/j.chom.2021.05.002
15. Seldin MM, Meng Y, Qi H, Zhu W, Wang Z, Hazen SL, Lusis AJ, Shih DM. Trimethylamine N-oxide promotes vascular inflammation through signaling of mitogen-activated protein kinase and nuclear factor- $\kappa$ B. *J Am Heart Assoc*. 2016;5:e002767. doi: 10.1161/jaha.115.002767
16. Li T, Chen Y, Gua C, Li X. Elevated circulating trimethylamine N-oxide levels contribute to endothelial dysfunction in aged rats through vascular inflammation and oxidative stress. *Front Physiol*. 2017;8:350. doi: 10.3389/fphys.2017.00350
17. Roberts AB, Gu X, Buffa JA, Hurd AG, Wang Z, Zhu W, Gupta N, Skye SM, Cody DB, Levison BS, et al. Development of a gut microbe-targeted non-lethal therapeutic to inhibit thrombosis potential. *Nat Med*. 2018;24:1407–1417. doi: 10.1038/s41591-018-0128-1
18. Organ CL, Otsuka H, Bhushan S, Wang Z, Bradley J, Trivedi R, Polhemus DJ, Tang WH, Wu Y, Hazen SL, et al. Choline diet and its gut microbe-derived metabolite, trimethylamine N-oxide, exacerbate pressure overload-induced heart failure. *Circ Heart Fail*. 2016;9:e002314. doi: 10.1161/CIRCHEARTFAILURE.115.002314
19. Boini KM, Hussain T, Li PL, Koka S. Trimethylamine-N-oxide instigates NLRP3 inflammasome activation and endothelial dysfunction. *Cell Physiol Biochem*. 2017;44:152–162. doi: 10.1159/000484623
20. Tang WH, Wang Z, Kennedy DJ, Wu Y, Buffa JA, Agatista-Boyle B, Li XS, Levison BS, Hazen SL. Gut microbiota-dependent trimethylamine N-oxide (TMAO) pathway contributes to both development of renal insufficiency and mortality risk in chronic kidney disease. *Circ Res*. 2015;116:448–455. doi: 10.1161/CIRCRESAHA.116.305360
21. Gupta N, Buffa JA, Roberts AB, Sangwan N, Skye SM, Li L, Ho KJ, Varga J, DiDonato JA, Tang WHW, et al. Targeted inhibition of gut microbial trimethylamine N-oxide production reduces renal tubulointerstitial fibrosis and functional impairment in a murine model of chronic kidney disease. *Arterioscler Thromb Vasc Biol*. 2020;40:1239–1255. doi: 10.1161/ATVBAHA.120.314139
22. Senthong V, Wang Z, Fan Y, Wu Y, Hazen SL, Tang WH. Trimethylamine N-oxide and mortality risk in patients with peripheral artery disease. *J Am Heart Assoc*. 2016;5:d004237. doi: 10.1161/JAHA.116.004237
23. Zeng Q, Rong Y, Li D, Wu Z, He Y, Zhang H, Huang L. Identification of serum biomarker in acute aortic dissection by global and targeted metabolomics. *Ann Vasc Surg*. 2020;68:497–504. doi: 10.1016/j.avsg.2020.06.026
24. Jiang S, Shui Y, Cui Y, Tang C, Wang X, Qiu X, Hu W, Fei L, Li Y, Zhang S, et al. Gut microbiota dependent trimethylamine N-oxide aggravates angiotensin II-induced hypertension. *Redox Biol*. 2021;46:102115. doi: 10.1016/j.redox.2021.102115
25. Karbach SH, Schönfelder T, Brandão I, Wilms E, Hörmann N, Jäckel S, Schüller R, Finger S, Knorr M, Lagrange J, et al. Gut microbiota promote angiotensin II-induced arterial hypertension and vascular dysfunction. *J Am Heart Assoc*. 2016;5:e003698. doi: 10.1161/jaha.116.003698
26. Jaworska K, Koper M, Ufnal M. Gut microbiota and renin-angiotensin system: a complex interplay at local and systemic levels. *Am J Physiol Gastrointest Liver Physiol*. 2021;321:G355–G366. doi: 10.1152/ajpgi.00099.2021
27. Xie J, Lu W, Zhong L, Hu Y, Li Q, Ding R, Zhong Z, Liu Z, Xiao H, Xie D, et al. Alterations in gut microbiota of abdominal aortic aneurysm mice. *BMC Cardiovasc Disord*. 2020;20:32. doi: 10.1186/s12872-020-01334-2
28. Daugherty A, Manning MW, Cassis LA. Angiotensin II promotes atherosclerotic lesions and aneurysms in apolipoprotein E-deficient mice. *J Clin Invest*. 2000;105:1605–1612. doi: 10.1172/JCI7818
29. Owens AP III, Edwards TL, Antoniak S, Geddings JE, Jahangir E, Wei WQ, Denny JC, Boulaftali Y, Bergmeier W, Daugherty A, et al. Platelet inhibitors reduce rupture in a mouse model of established abdominal aortic aneurysm. *Arterioscler Thromb Vasc Biol*. 2015;35:2032–2041. doi: 10.1161/ATVBAHA.115.305537
30. Craciun S, Balskus EP. Microbial conversion of choline to trimethylamine requires a glycyl radical enzyme. *Proc Natl Acad Sci USA*. 2012;109:21307–21312. doi: 10.1073/pnas.1215689109
31. Romano KA, Vivas EI, Amador-Noguez D, Rey FE. Intestinal microbiota composition modulates choline bioavailability from diet and accumulation of the proatherogenic metabolite trimethylamine-N-oxide. *mBio*. 2015;6:e02481. doi: 10.1128/mBio.02481-14
32. Bennett BJ, de Aguiar Vallim TQ, Wang Z, Shih DM, Meng Y, Gregory J, Allayee H, Lee R, Graham M, Crooke R, et al. Trimethylamine-N-oxide, a metabolite associated with atherosclerosis, exhibits complex genetic and dietary regulation. *Cell Metab*. 2013;17:49–60. doi: 10.1016/j.cmet.2012.12.011
33. Schugar RC, Shih DM, Warrier M, Helsley RN, Burrows A, Ferguson D, Brown AL, Gromovsky AD, Heine M, Chatterjee A, et al. The TMAO-producing enzyme flavin-containing monooxygenase 3 regulates obesity and the beiging of white adipose tissue. *Cell Rep*. 2017;19:2451–2461. doi: 10.1016/j.celrep.2017.05.077
34. Chen S, Henderson A, Petriello MC, Romano KA, Gearing M, Miao J, Schell M, Sandoval-Espinola WJ, Tao J, Sha B, et al. Trimethylamine N-oxide binds and activates PERK to promote metabolic dysfunction. *Cell Metab*. 2019;30:1141–1151.e5. doi: 10.1016/j.cmet.2019.08.021
35. Rowe VL, Stevens SL, Reddick TT, Freeman MB, Donnell R, Carroll RC, Goldman MH. Vascular smooth muscle cell apoptosis in aneurysmal, occlusive, and normal human aortas. *J Vasc Surg*. 2000;31:567–576.
36. Hu J, Xu J, Shen S, Zhang W, Chen H, Sun X, Qi Y, Zhang Y, Zhang Q, Guo M, et al. Trimethylamine N-oxide promotes abdominal aortic aneurysm formation by aggravating aortic smooth muscle cell senescence in mice. *J Cardiovasc Transl Res*. 2022;15:1064–1074. doi: 10.1007/s12265-022-10211-6
37. Golledge J. Abdominal aortic aneurysm: update on pathogenesis and medical treatments. *Nat Rev Cardiol*. 2019;16:225–242. doi: 10.1038/s41569-018-0114-9
38. Manning MW, Cassis LA, Daugherty A. Differential effects of doxycycline, a broad-spectrum matrix metalloproteinase inhibitor, on angiotensin II-induced atherosclerosis and abdominal aortic aneurysms. *Arterioscler Thromb Vasc Biol*. 2003;23:483–488. doi: 10.1161/01.ATV.0000058404.92759.32
39. Baxter BT, Matsumura J, Curci JA, McBride R, Larson L, Blackwelder W, Lam D, Wijesinha M, Terrin M; N-TA3CT Investigators. Effect of doxycycline on aneurysm growth among patients with small infrarenal abdominal aortic aneurysms: a randomized clinical trial. *JAMA*. 2020;323:2029–2038. doi: 10.1001/jama.2020.5230
40. Chen ML, Zhu XH, Ran L, Lang HD, Yi L, Mi MT. Trimethylamine-N-oxide induces vascular inflammation by activating the NLRP3 inflammasome through the SIRT3-SOD2-mtROS signaling pathway. *J Am Heart Assoc*. 2017;6:e006347. doi: 10.1161/jaha.117.006347
41. King VL, Trivedi DB, Gitlin JM, Loftin CD. Selective cyclooxygenase-2 inhibition with celecoxib decreases angiotensin II-induced abdominal aortic aneurysm formation in mice. *Arterioscler Thromb Vasc Biol*. 2006;26:1137–1143. doi: 10.1161/01.ATV.0000216119.79008.ac
42. Xiong W, MacTaggart J, Knispel R, Worth J, Persidsky Y, Baxter BT. Blocking TNF- $\alpha$  attenuates aneurysm formation in a murine model. *J Immunol*. 2009;183:2741–2746. doi: 10.4049/jimmunol.0803164
43. Shi J, Guo J, Li Z, Xu B, Miyata M. Importance of NLRP3 inflammasome in abdominal aortic aneurysms. *J Atheroscler Thromb*. 2021;28:454–466. doi: 10.5551/jat.RV17048
44. Zhang X, Thatcher SE, Rateri DL, Brummer D, Charnigo R, Daugherty A, Cassis LA. Transient exposure of neonatal female mice to testosterone abrogates the sexual dimorphism of abdominal aortic aneurysms. *Circ Res*. 2012;110:e73–e85. doi: 10.1161/CIRCRESAHA.111.253880
45. Alsiraj Y, Thatcher SE, Charnigo R, Chen K, Blalock E, Daugherty A, Cassis LA. Female mice with an XY sex chromosome complement develop severe angiotensin II-induced abdominal aortic aneurysms. *Circulation*. 2017;135:379–391. doi: 10.1161/CIRCULATIONAHA.116.023789
46. Sawada H, Lu HS, Cassis LA, Daugherty A. Twenty years of studying AngII (angiotensin II)-induced abdominal aortic pathologies in

mice: continuing questions and challenges to provide insight into the human disease. *Arterioscler Thromb Vasc Biol*. 2022;42:277–288. doi: 10.1161/ATVBAHA.121.317058

47. Wang M, Kaufman RJ. Protein misfolding in the endoplasmic reticulum as a conduit to human disease. *Nature*. 2016;529:326–335. doi: 10.1038/nature17041
48. Li Y, Lu G, Sun D, Zuo H, Wang DW, Yan J. Inhibition of endoplasmic reticulum stress signaling pathway: a new mechanism of statins to suppress the development of abdominal aortic aneurysm. *PLoS One*. 2017;12:e0174821. doi: 10.1371/journal.pone.0174821
49. Navas-Madronal M, Rodriguez C, Kassan M, Fite J, Escudero JR, Canes L, Martinez-Gonzalez J, Camacho M, Galan M. Enhanced endoplasmic reticulum and mitochondrial stress in abdominal aortic aneurysm. *Clin Sci (Lond)*. 2019;133:1421–1438. doi: 10.1042/CS20190399
50. López-Candales A, Holmes DR, Liao S, Scott MJ, Wickline SA, Thompson RW. Decreased vascular smooth muscle cell density in medial degeneration of human abdominal aortic aneurysms. *Am J Pathol*. 1997;150:993–1007.
51. Hu H, Tian M, Ding C, Yu S. The C/EBP homologous protein (CHOP) transcription factor functions in endoplasmic reticulum stress-induced apoptosis and microbial infection. *Front Immunol*. 2018;9:3083. doi: 10.3389/fimmu.2018.03083
52. Kalnins G, Kuka J, Grinberga S, Makrecka-Kuka M, Liepinsh E, Dambrova M, Tars K. Structure and function of CutC choline lyase from human microbiota bacterium *Klebsiella pneumoniae*. *J Biol Chem*. 2015;290:21732–21740. doi: 10.1074/jbc.M115.670471
53. Gomaa EZ. Human gut microbiota/microbiome in health and diseases: a review. *Antonie Van Leeuwenhoek*. 2020;113:2019–2040. doi: 10.1007/s10482-020-01474-7
54. Ezeji JC, Sarikonda DK, Hopperton A, Erkkila HL, Cohen DE, Martinez SP, Cominelli F, Kuwahara T, Dichosa AEK, Good CE, et al. *Parabacteroides distasonis*: intriguing aerotolerant gut anaerobe with emerging antimicrobial resistance and pathogenic and probiotic roles in human health. *Gut Microbes*. 2021;13:1922241. doi: 10.1080/19490976.2021.1922241
55. Gan XT, Ettinger G, Huang CX, Burton JP, Haist JV, Rajapurohitam V, Sidaway JE, Martin G, Gloor GB, Swann JR, et al. Probiotic administration attenuates myocardial hypertrophy and heart failure after myocardial infarction in the rat. *Circ Heart Fail*. 2014;7:491–499. doi: 10.1161/CIRCHEARTFAILURE.113.000978
56. Hu J, Xu J, Shen S, Zhang W, Chen H, Sun X, Qi Y, Zhang Y, Zhang Q, Guo M, et al. Trimethylamine N-oxide promotes abdominal aortic aneurysm formation by aggravating aortic smooth muscle cell senescence in mice. *J Cardiovasc Transl Res*. 2022;15:1064–1074. doi: 10.1007/s12265-022-10211-6
57. Raffetto JD, Leverkus M, Park HY, Menzoian JO. Synopsis on cellular senescence and apoptosis. *J Vasc Surg*. 2001;34:173–177. doi: 10.1067/mva.2001.115964
58. Quintana RA, Taylor WR. Cellular mechanisms of aortic aneurysm formation. *Circ Res*. 2019;124:607–618. doi: 10.1161/CIRCRESAHA.118.313187
59. Sundermann AC, Saum K, Conrad KA, Russell HM, Edwards TL, Mani K, Björck M, Wanhainen A, Owens AP 3rd. Prognostic value of D-dimer and markers of coagulation for stratification of abdominal aortic aneurysm growth. *Blood Adv*. 2018;2:3088–3096. doi: 10.1182/bloodadvances.2017013359
60. Wanhainen A, Mani K, Vorkapic E, De Basso R, Björck M, Lanne T, Wagsater D. Screening of circulating microRNA biomarkers for prevalence of abdominal aortic aneurysm and aneurysm growth. *Atherosclerosis*. 2017;256:82–88. doi: 10.1016/j.atherosclerosis.2016.11.007
61. Lu G, Su G, Davis JP, Schaheen B, Downs E, Roy RJ, Ailawadi G, Upchurch GR Jr. A novel chronic advanced stage abdominal aortic aneurysm murine model. *J Vasc Surg*. 2017;66:232–242.e4. doi: 10.1016/j.jvs.2016.07.105
62. Berman AG, Romary DJ, Kerr KE, Gorazd NE, Wigand MM, Patnaik SS, Finol EA, Cox AD, Goergen CJ. Experimental aortic aneurysm severity and growth depend on topical elastase concentration and lysyl oxidase inhibition. *Sci Rep*. 2022;12:99. doi: 10.1038/s41598-021-04089-8
63. Wang Z, Levison BS, Hazen JE, Donahue L, Li XM, Hazen SL. Measurement of trimethylamine-N-oxide by stable isotope dilution liquid chromatography tandem mass spectrometry. *Anal Biochem*. 2014;455:35–40. doi: 10.1016/j.ab.2014.03.016
64. Caporaso JG, Kuczynski J, Stombaugh J, Bittinger K, Bushman FD, Costello EK, Fierer N, Pena AG, Goodrich JK, Gordon JL, et al. QIIME allows analysis of high-throughput community sequencing data. *Nat Methods*. 2010;7:335–336. doi: 10.1038/nmeth.f.303
65. Callahan BJ, McMurdie PJ, Rosen MJ, Han AW, Johnson AJ, Holmes SP. DADA2: high-resolution sample inference from Illumina amplicon data. *Nat Methods*. 2016;13:581–583. doi: 10.1038/nmeth.3869
66. McMurdie PJ, Holmes S. phyloseq: An R package for reproducible interactive analysis and graphics of microbiome census data. *PLoS One*. 2013;8:e61217. doi: 10.1371/journal.pone.0061217
67. McMurdie PJ, Holmes S. Waste not, want not: why rarefying microbiome data is inadmissible. *PLoS Comput Biol*. 2014;10:e1003531. doi: 10.1371/journal.pcbi.1003531
68. Wickham H. *ggplot2: Elegant Graphics for Data Analysis*. Springer Publishing Co, Inc; 2009.
69. Benjamini Y. Discovering the false discovery rate. *J Royal Stat Soc Series B (Stat Method)*. 2010;72:405–416. doi: 10.1111/j.1467-9868.2010.00746.x
70. Hollander M, Wolfe DAW. *Nonparametric Statistical Methods*. Wiley; 1999.
71. Rivero-Gutiérrez B, Anzola A, Martínez-Augustín O, de Medina FS. Stain-free detection as loading control alternative to Ponceau and house-keeping protein immunodetection in Western blotting. *Anal Biochem*. 2014;467:1–3. doi: 10.1016/j.ab.2014.08.027